AD-A038 562 HONEYWELL INC MINNEAPOLIS MINN GOVERNMENT AND AERONA--ETC F/G 20/4
PRODUCTION SUITABILITY OF AN ELECTROFORM CONDUCTIVE-WAX PROCESS--ETC(U)
APR 77 W POSINGIES DAAJ02-74-C-0012
UNCLASSIFIED USAAMRDL-TR-77-2 NL

1 OF 1
ADA038562

ADA038562

USAAMRDL-TR-77-2

12

PRODUCTION SUITABILITY OF AN ELECTROFORM CONDUCTIVE - WAX PROCESS FOR THE MANUFACTURE OF FLUIDIC SYSTEMS

Honeywell Inc.
Government and Aeronautical Products Division
Minneapolis, Minn. 55413

April 1977

Final Report for Period March 1976 - October 1976

Approved for public release;
distribution unlimited.

Prepared for

U. S. ARMY AVIATION SYSTEMS COMMAND
P. O. Box 209
St. Louis, Mo. 63166

EUSTIS DIRECTORATE
U. S. ARMY AIR MOBILITY RESEARCH AND DEVELOPMENT LABORATORY
Fort Eustis, Va. 23604

EUSTIS DIRECTORATE POSITION STATEMENT

This report covers Phase III of a three-phase program to determine and demonstrate the production suitability of the Electroform Conductive Wax (ECW) process, used in conjunction with existing, conventional processes, for the manufacture of fluidic systems. During Phase III, a small production run, consisting of 20 Hydrofluidic Stability Augmentation Systems, was accomplished with production-oriented personnel operating the production line established during Phases I and II of this program. All components were completely tested and then randomly assembled into systems. These systems were then evaluated, and the test data was documented. The data derived during this program was used to project manufacturing costs, including nonrecurring costs, for quantities of 50 and 1,000 Hydrofluidic Stability Augmentation Systems.

Mr. George W. Fosdick of the Systems Support Division of the Eustis Directorate served as the project engineer for this effort.

UNCLASSIFIED

SECURITY CLASSIFICATION OF THIS PAGE (WHEN DATA ENTERED)

REPORT DOCUMENTATION PAGE | **READ INSTRUCTIONS BEFORE COMPLETING FORM**

18

1. REPORT NUMBER 19
USAAMRDL-TR-77-2

2. GOV'T ACCESSION NUMBER

3. RECIPIENT'S CATALOG NUMBER
9

6

4. TITLE (AND SUBTITLE)
PRODUCTION SUITABILITY OF AN ELECTROFORM CONDUCTIVE-WAX PROCESS FOR THE MANUFACTURE OF FLUIDIC SYSTEMS

5. TYPE OF REPORT/PERIOD COVERED
Final Report,
Marc[redacted] — Oct[redacted]76

6. PERFORMING ORG. REPORT NUMBER

10

7. AUTHOR(S)
Walter/Posingies

15

8. CONTRACT OR GRANT NUMBER(S)
DAAJ02-74-C-0012

9. PERFORMING ORGANIZATIONS NAME/ADDRESS
Honeywell Inc.
Government and Aeronautical Products Division
Minneapolis, Minnesota 55413

10. PROGRAM ELEMENT,PROJECT,TASK AREA & WORK UNIT NUMBERS
9841692000
98L(1)69 2000, 74004

11. CONTROLLING OFFICE NAME/ADDRESS
U.S. Army Aviation Systems Command
P.O. Box 209, Main Office
St. Louis, Missouri 63166

11

12. REPORT DATE
Apr[redacted]977

12 96p.

13. NUMBER OF PAGES
95

14. MONITORING AGENCY NAME/ADDRESS (IF DIFFERENT FROM CONT. OFF.)
Eustis Directorate
U.S. Army Air Mobility R&D Laboratory
Fort Eustis, Virginia 23604

15. SECURITY CLASSIFICATION (OF THIS REPORT)
UNCLASSIFIED

15a. DECLASSIFICATION DOWNGRADING SCHEDULE

16. DISTRIBUTION STATEMENT (OF THIS REPORT)

Approved for public release; distribution unlimited.

17. DISTRIBUTION STATEMENT (OF THE ABSTRACT ENTERED IN BLOCK 20, IF DIFFERENT FROM REPORT)

18. SUPPLEMENTARY NOTES

19. KEY WORDS (CONTINUE ON REVERSE SIDE IF NECESSARY AND IDENTIFY BY BLOCK NUMBER)

Hydrofluidics
Electroforming
Conductive Wax
Production Process

20. ABSTRACT (CONTINUE ON REVERSE SIDE IF NECESSARY AND IDENTIFY BY BLOCK NUMBER)

This document presents the results of Phase III of a three-phase program to determine and demonstrate the suitability of the electroform conductive-wax process, used in conjunction with conventional production processes, for the manufacture of fluidic systems. During Phase I, an integrated amplifier-manifold hydrofluidic stability augmentation system using the electroform conductive wax process was successfully designed, fabricated, and qualification tested, and a pilot production line using the electroform conductive wax process was defined. The pilot production line includes over

HD-168 REV 11/74

DD FORM 1 JAN 73 1473 EDITION OF 1 NOV 55 IS OBSOLETE

UNCLASSIFIED

SECURITY CLASSIFICATION OF THIS PAGE (WHEN DATA ENTERED)

406 808

20. Abstract (continued)

all manufacturing, inspection, and assembly equipment necessary to produce the integrated amplifier-manifold hydrofluidic stability augmentation systems. Phase II included the setup and checkout of the pilot production line. Three groups of three systems each were fabricated and tested. Circuit configuration and the production processes were changed as a result of the analysis of each group of components. In this phase, Phase III, a small "proof" production run was accomplished, using the pilot production line and the revised production process. Component quality was determined through detailed testing of components and systems combined with statistical analysis. A complete definition of the hardware was defined in a separately submitted technical data package.

2

TABLE OF CONTENTS

LIST OF ILLUSTRATIONS

LIST OF TABLES

LIST OF TABLES (Continued)

LIST OF TABLES (Concluded)

SECTION I
INTRODUCTION

Most conventional production techniques are not readily adaptable to the manufacture of fluidic devices with small passageways, intricate configurations, close-tolerance requirements, and the need for sealed circuits. Consequently, the electroform conductive-wax (ECW) process was developed. Through various developmental programs, it was demonstrated that the ECW process has the capability for accurately fabricating leak-proof fluidic components. The object of this program is to determine the production suitability of the ECW process, in conjunction with existing conventional processes, for the manufacture of fluidic systems. This 34-month program was divided into three phases. Phase I, reported in USAAMRDL-TR-75-49, consisted of the following major tasks:[1]

- Design and development of an integrated amplifier-manifold circuit for use in the hydrofluidic yaw axis stability augmentation system (SAS), which was developed under Contract DAAJ02-72-C-0051 for the Eustis Directorate, USAAMRDL, Fort Eustis, Virginia.

- Qualification testing of the SAS with the integrated amplifier-manifold circuit.

---

1 Robert Lewis, Walter Posingies, and Burton Scott, Production Suitability of an Electroform Conductive Wax Process For the Manufacture of Fluidic Systems, Honeywell Inc., USAAMRDL Technical Report 75-49, Eustis Directorate, U. S. Army Air Mobility Research and Development Laboratory, Fort Eustis, Virginia, November 1975, AD A018874.

- Design of a pilot production line for the fabrication of fluidic components using the ECW process and for the functional testing of the components.

Phase II, reported in USAAMRDL-TR-76-42, consisted of the following major tasks:[2]

- Manufacture, assembly, and checkout of the complete production line designed in Phase I.
- Fabrication and testing of three lots of system components using the Phase I production line. Each lot consisted of three sets of hardware.
- Assembly and testing of a complete system from each lot.
- Analysis of the test results of each lot to modify the design, the ECW process, or process equipment, if necessary, before fabrication of the next lot.

Phase III, the subject of this report, consisted of the following major tasks:

- Fabrication of four lots of electroformed components, each lot consisting of five sets of components.
- Testing of all electroformed components, flow-control valves, and pilot input device (PID) valves as components, and evaluating them after they had been randomly assembled into systems.

---

[2] Walter Posingies, Production Suitability of an Electroform Conductive Wax Process for the Manufacture of Fluidic Systems, Honeywell Inc., USAAMRDL Technical Report 76-42, Eustis Directorate, U.S. Army Air Mobility Research and Development Laboratory, Fort Eustis, Virginia, July 1976.

- Application of statistical analysis to the component test data to develop statistical distributions and performance variances.

- Calculation of projected manufacturing cost, which included nonrecurring costs, for quantities of 50 and 1000 systems.

SECTION II
SYSTEM CONFIGURATION

A photograph of a completed yaw axis fluidic controller is shown in Figure 1. This system is designed to bolt directly onto a Hydraulic Research 30005000 servoactuator. Input flow is supplied by the servoactuator in the location shown, and signals generated within the controller are communicated back through the three servo command ports in the outlet block. Also shown in this photograph is the flow-control valve, which maintains fluidic system flow at 0.7 gpm over the fluid temperature range from 40°F to 180°F.

Output commands are computed by the fluidic controller using both its internal vortex rate gyro and a second device that transduces pilot yaw commands into fluidic signals (PID). The PID input cable and PID level arm are also labeled in Figure 1. Relationships between these components are shown in the Figure 2 schematic.

Resistors R22 and R23 in the schematic are the electroformed bolt-on through-rate resistors shown in Figure 1. Electroformed bolt-on feedback resistors, R10 and R11, and the viscosity-sensitive bypass resistor are in both figures. Another feature visible in the photograph is the dual-function lock lever, which rotates a blade within the vortex chamber to generate a swirl similar to that produced by input turning rates. This lever can be adjusted to compensate for rate sensor offsets during calibration and can be pushed to generate a "psuedo-rate", providing a built-in test (BIT) function during system performance checkout in the aircraft.

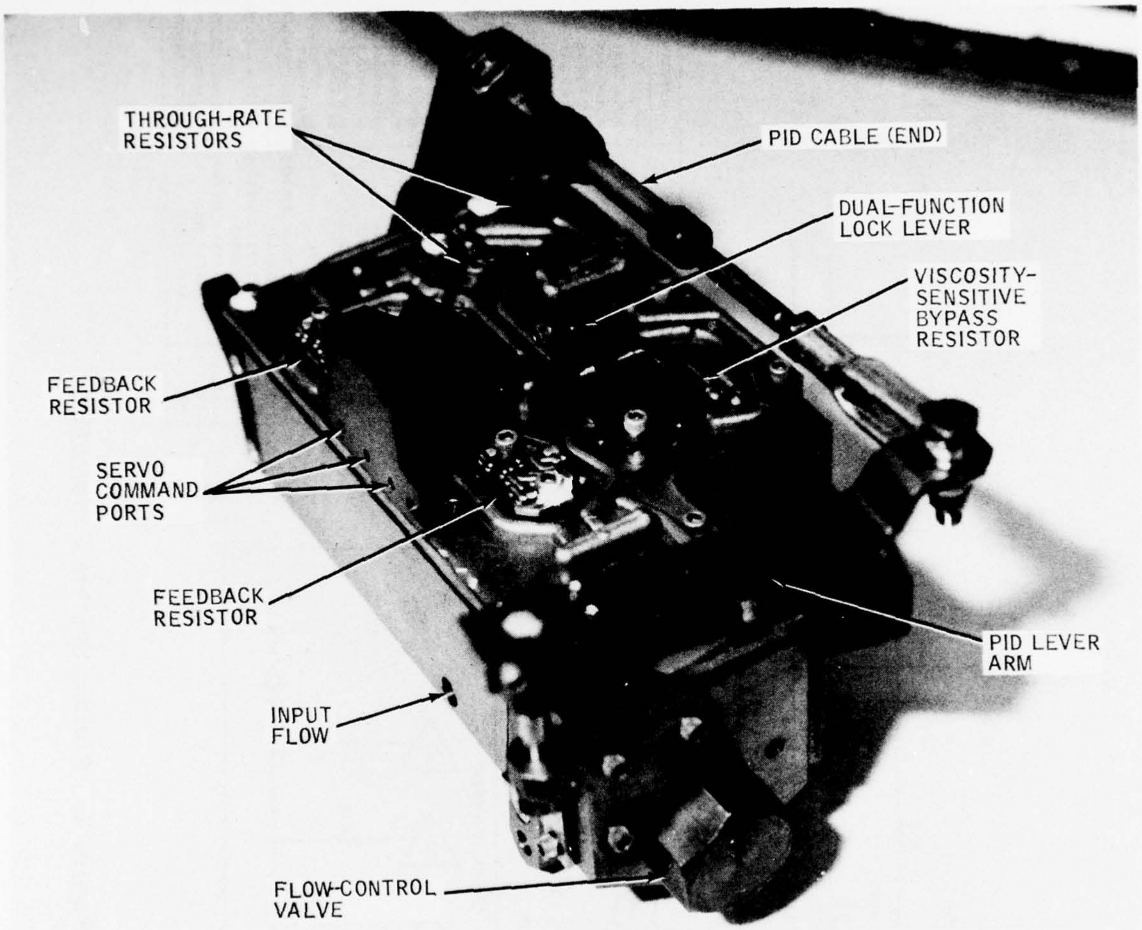

Figure 1. Yaw Axis Fluidic Controller.

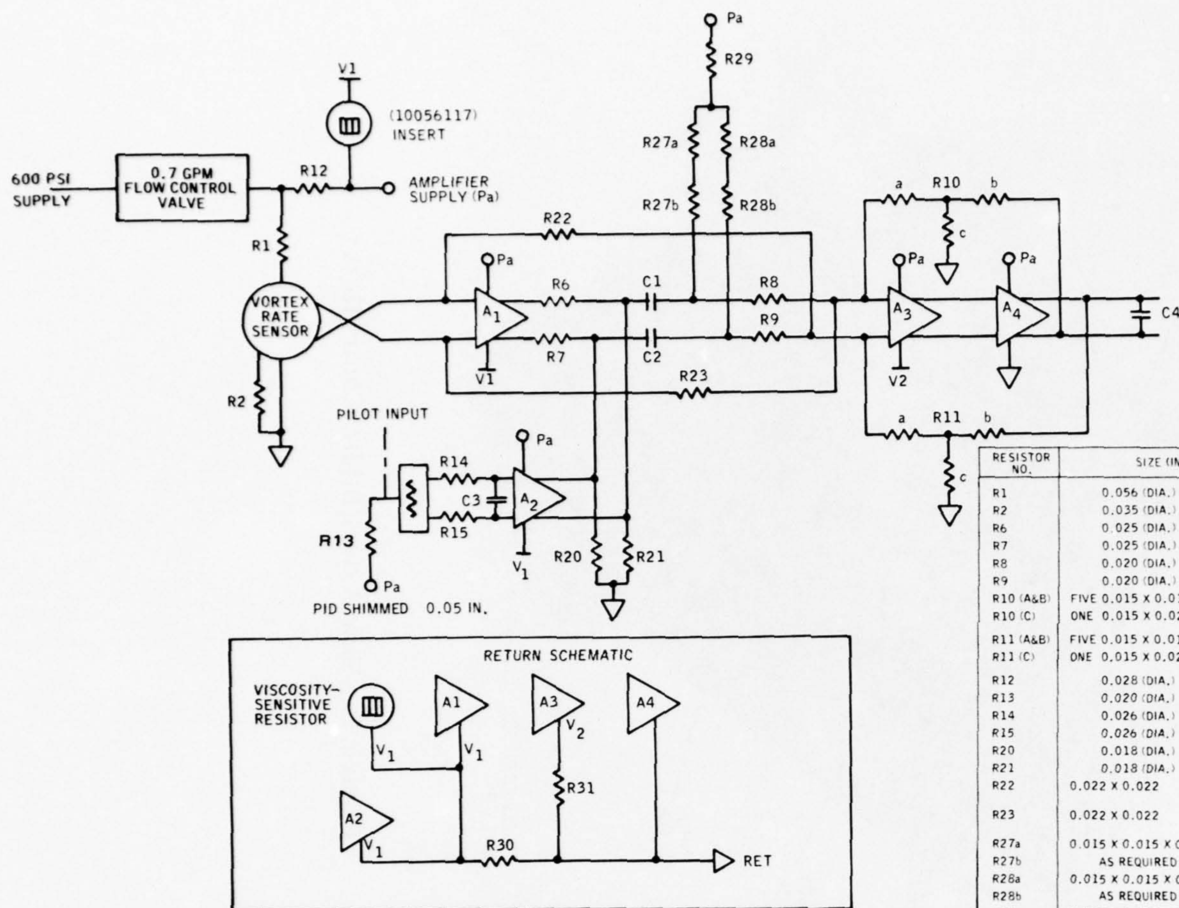

RESISTOR NO.	SIZE (IN.)	CONFIGURATION
R1	0.056 (DIA.)	DRILLED IN HOUSING
R2	0.035 (DIA.)	REPLACEABLE
R6	0.025 (DIA.)	REPLACEABLE
R7	0.025 (DIA.)	REPLACEABLE
R8	0.020 (DIA.)	REPLACEABLE
R9	0.020 (DIA.)	REPLACEABLE
R10 (A&B)	FIVE 0.015 X 0.015 IN SERIES	THREE BRANCH NETWORK ELECTROFORMED AS A BOLT ON ASSEMBLY
R10 (C)	ONE 0.015 X 0.023	
R11 (A&B)	FIVE 0.015 X 0.015 IN SERIES	THREE BRANCH NETWORK ELECTROFORMED AS A BOLT ON ASSEMBLY
R11 (C)	ONE 0.015 X 0.023	
R12	0.028 (DIA.)	REPLACEABLE
R13	0.020 (DIA.)	REPLACEABLE
R14	0.026 (DIA.)	REPLACEABLE
R15	0.026 (DIA.)	REPLACEABLE
R20	0.018 (DIA.)	REPLACEABLE
R21	0.018 (DIA.)	REPLACEABLE
R22	0.022 X 0.022	ELECTROFORMED BOLT ON ASSEMBLY
R23	0.022 X 0.022	ELECTROFORMED BOLT ON ASSEMBLY
R27a	0.015 X 0.015 X 0.070 LONG	ELECTROFORMED ON IC
R27b	AS REQUIRED	REPLACEABLE
R28a	0.015 X 0.015 X 0.070 LONG	ELECTROFORMED ON IC
R28b	AS REQUIRED	REPLACEABLE
R29	0.015 X 0.015 X 0.020 LONG	ELECTROFORMED ON IC
R30	0.047 X 0.050	ELECTROFORMED ON IC
R31	0.027 X 0.027	ELECTROFORMED ON IC

Figure 2. Fluidic System Schematic.

Figure 3 is an exploded view of the controller hardware with the major components labeled. Amplifier-manifold is the official name for the integrated circuit, which is the largest and most complex electroformed component on this program. The BIT blade can be observed protruding through the rate sensor cover. High-pass capacitors are bellows soldered to covers and are labeled C1 and C2 in the schematic. Other capacitors are the lag capacitor, C3, and the filter capacitor, C4. An electroformed pickoff combined with a stack of etched coupling-element disks constitute the pickoff assembly. Figure 4 is an assembly drawing showing details of controller construction, and Table 1 is a parts list.

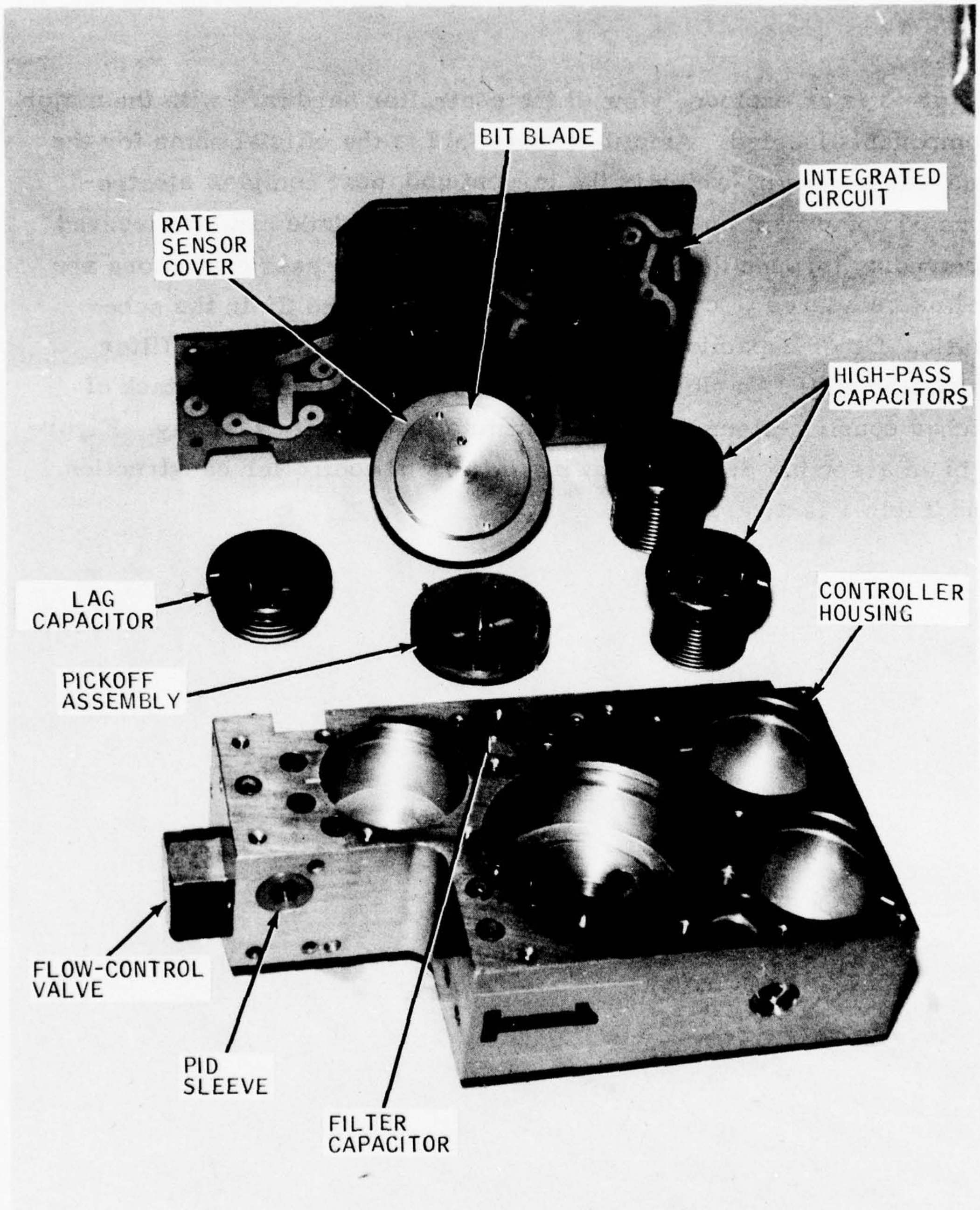

Figure 3. Yaw Controller -- Exploded View.

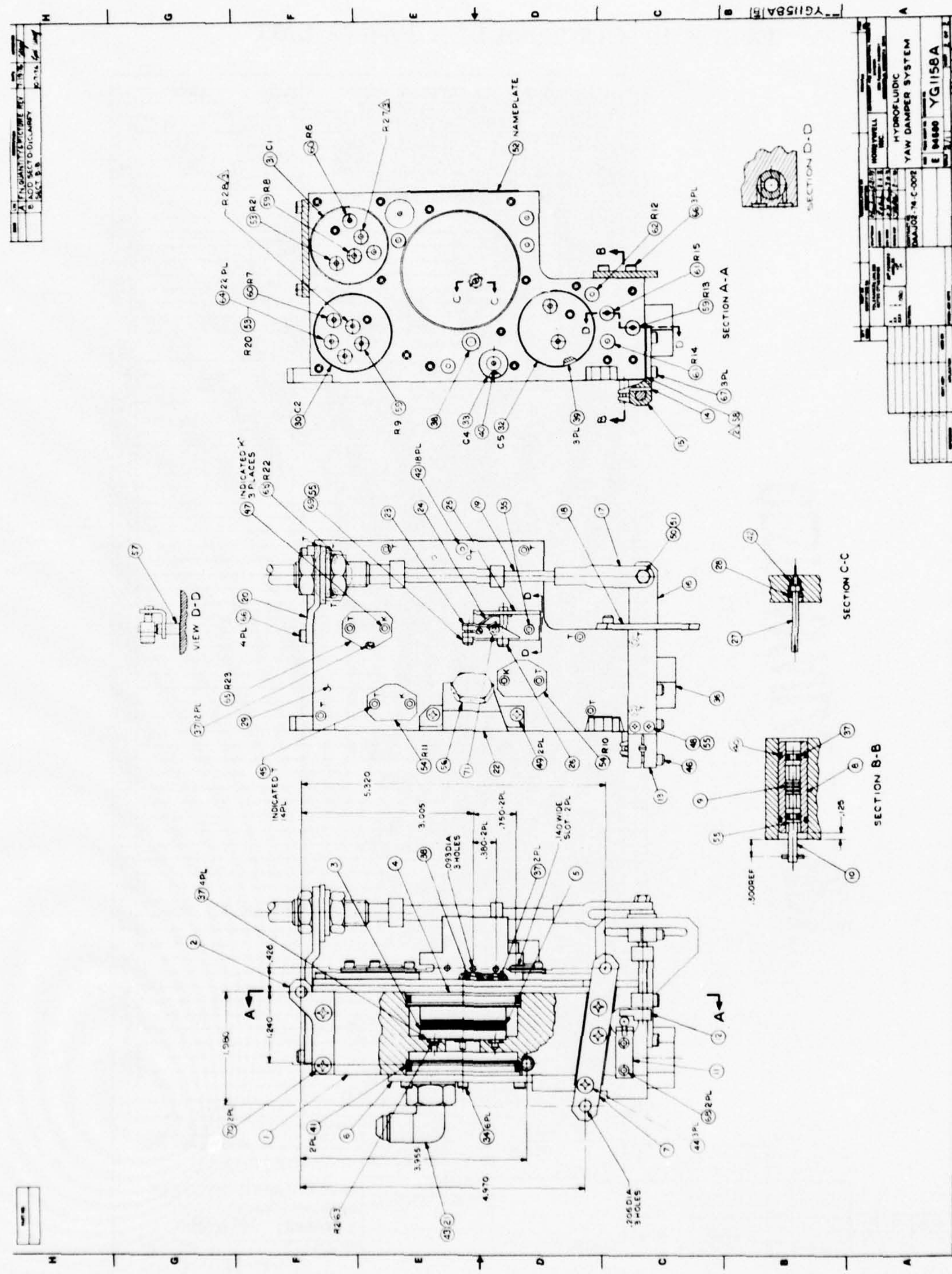

Figure 4. Hydrofluidic Yaw Damper System.

TABLE 1. CONTROLLER PARTS LIST

QTY REQD	PART OR IDENTIFYING NO.	NOMENCLATURE OR DESCRIPTION	REMARKS	ITEM NO.
1	NAS1352C04-8	SCREW, CAP, SOCKET HEAD	4-40 × .5 CRES	71
2	MS24693-C26	SCREW MACHINE FLAT HEAD	6-32 × .375	70
1	NAS1352-04-4P	SCREW CAP SOCKET HEAD	4-40 × 25 CAD PL	69
2	NAS1352C04-4	SCREW, CAP SOCKET HEAD	4-40 × 25 CRES	68
3	NAS1352C04-5	SCREW CAP SOCKET HEAD	4-40 × .31 CRES	67
7	NAS1352C04-6	SCREW CAP SOCKET HEAD	4-40 × 37 CRES	66
2	10050020-102	MANIFOLD ASSEMBLY	R22, R23	65
22	MS28775-006	PACKING, PREFORMED HYD		64
1	10047089-118	ORIFICE	R2	63
1	10047089-133	ORIFICE	R12	62
2	10047089-110	ORIFICE	R14, R15	61
2	10047089-109	ORIFICE	R6, R7	60
3	10047089-106	ORIFICE	R8, R9, R13	59
AR	10058163-XXX	SHIM	-101, -102, -103	58
2	NAS43DD0-16	SPACER, SCREW AND BOLT	.25 LONG	57
1	AN814-5D	PLUG AND BLEEDER		56
AR	GRADE C	SEALING COMPOUND	MIL-S-22473	55
2	10050020-101	MANIFOLD ASSEMBLY	R10, R11	54
2	10047089-105	ORIFICE	R20, R21	53
1	10058167-101	PLATE, IDENTIFICATION		52
1	NAS1291C3	NUT, SELF LOCKING	10-32 800°F	51
1	AN3C6	BOLT, MACHINE, AIRCRAFT	10-32 × .75	50
2	MS24693-C6	SCREW, MACHINE, FLAT HEAD	4-40 × 5	49
2	NAS662C2R4	SCREW, MACHINE FLAT HEAD	2-56 × .25 100° CTSK	48
3	NAS1352-04-10P	SCREW, CAP, SOCKET HEAD	4-40 × .625 CAD PL	47
1	NAS1352-04-8P	SCREW CAP SOCKET HEAD	4-40 × .50 CAD PL	46
14	NAS1352-04-6P	SCREW, CAP, SOCKET HEAD	4-40 × .375 CAD PL	45
3	MS24693-C27	SCREW, MACHINE FLAT HD	6-32 × .437	44
1	MS28775-5	PACKING, PREFORMED HYD		43
1	MS28775-004	PACKING, PREFORMED HYD		42
2	MS28775-133	PACKING, PREFORMED HYD		41
4	MS28775-012	PACKING, PREFORMED, HYD		40
3	MS28775-025	PACKING, PREFORMED, HYD		39
12	MS28775-008	PACKING, PREFORMED HYD		38
18	MS28775-005	PACKING, PREFORMED, HYD		37
1	10047182-101	VALVE, FLOW CONTROL		36
1	NAS1352-04-12	SCREW CAP SOCKET HEAD	4-40 × .75	35
6	NAS1352-06-6	SCREW, CAP SOCKET HEAD	6-32 × .375	34
1	10050030-101	BELLOWS ASSY	C4	33
1	10050026-103	BELLOWS ASSY	C5	32
1	10050026-101	BELLOWS ASSY	C1	31
1	10050026-102	BELLOWS ASSY	C2	30
1	10050022-101	AMPLIFIER, MANIFOLD		29
1	10040763-101	SLEEVE, LOCKING		28
1	10040762-103	PIN, NULL ADJ		27
1	10058164-101	SCREW, SHOULDER		26
1	10050032-101	BRACKET, NULL ADJUST		25
1	10049202-101	SPRING		24
1	10047435-101	LOCK LEVER, NULL		23
1	10050024-101	BLOCK OUTLET		22
1	MS51527B5	ELBOW		21
1	10050039-101	BRACKET, CABLE		20
1	10047183-101	CABLE, PUSH PULL		19
1	10047444-101	BRACKET SUPPORT		18
1	MS35812-1	CLEVIS		17
1	10047443-101	ARM, SPOOL ADJ		16
1	10050040-101	PLATE, PIVOT		15
1	MS16555-604	PIN, STRAIGHT (DOWEL)	.062 DIA × .375 LONG	14
1	10049198-101	CLEVIS, ADJUSTMENT		13
1	10047440-101	PIN SPOOL LINK		12
1	10049570-101	GUIDE		11
1	10047441-101	PIN, SPOOL END		10
1	10040250-101	SPOOL		9
1	10040251-101	SLEEVE		8
1	10049200-101	BAR, MOUNTING		7
1	10050036-101	COVER, VRS BOTTOM		6
34	10040030-101	COUPLING ELEMENT		5
1	10052137-101	COVER, VRS TOP		4
1	10058162-101	PICKOFF ASSEMBLY		3
1	10050038-101	HANGER, MOUNTING		2
1	10050025-101	HOUSING, CONTROLLER		1

TOLERANCES UNLESS NOTED OTHERWISE
X ±
XX ±
XXX ±.020
90° FORMED ANGLES ±2° 1°

DRAFTSMAN Brand 7-16-76
CHECKER 8-6-76
DEV ENGR 7-9-76
ENGRG MGT

MATERIAL

CONTRACT NO. DAAJ02-74-C-0012

FINISH SEE NOTE

HONEYWELL INC.
GOVERNMENT AND AERONAUTICAL PRODUCTS DIVISION
2600 RIDGWAY PARKWAY
MINNEAPOLIS, MINNESOTA 55413

HYDROFLUIDIC YAW DAMPER SYSTEM

SIZE E | CODE IDENT NO. 94580 | DRAWING NO. YG1158A

SCALE 2/1 | SHEET 1 OF 2

CONTROL A

NEXT ASSY | USED ON

APPLICATION

REFERENCE

B	B	REV
2	1	SHEET

SECTION III
COMPONENT FABRICATION AND TEST

Electroformed components were fabricated in four lots of five components each in accordance with the process defined in Phase II of this contract. Each system contains the following electroformed components:

- One rate-sensor pickoff
- One integrated circuit (IC)
- One set of through-rate resistors
- One set of feedback resistors

Two of the nonelectroformed components were calibrated. They are:

- PID valve assembly
- Flow-control valve

RATE SENSORS

Three lots of rate-sensor pickoffs were rejected based on visual inspection prior to testing. The entire lots were rejected even though some of the sensors appeared to be satisfactory.

Thin plating in critical areas of the original, Lot A pickoffs was caused by an excessive plating current density. The pickoff was plated at twice the specified current density due to some error in following the production procedure or to some problem with the production setup.

Air-bubble accumulations on Lot B rate sensors occurred in the same critical area and also resulted in several unsatisfactory pickoffs.

Because the production process could not change in the middle of the production run, it was necessary to scrap the entire two lots, revise the process, and start over. Instrumentation was recalibrated, and plating currents were set more accurately to ensure that the excessive current condition would not occur again. The procedure was also changed to include a "flushing" step to remove bubbles from the pick-off.

The revised process was satisfactory for the next three lots; however, the initial problem of thin plating recurred in the final lot. Test data taken during the second attempt to plate Lot D indicated that the plating anode impedance was increasing as a function of time. Only 1 volt was required to obtain the 0.6-amp plating current at the start, for an effective impedance of 1.67 ohm. This impedance had increased to 3.4 ohms several hours later and was up to 6.67 ohms by the end of the day. Voltage and current were monitored only during working hours. The load-sensitive power supply used will vary plating current as the impedance changes unless it is readjusted.

Plating thickness on the second Lot D was satisfactory, and further investigations into the plating problem were not undertaken. Recommendations for future rate-sensor manufacturing runs are given below.

- Record plating current (and voltage if practical) continuously during the 48-hour plating period, using a slow-speed strip-chart or circular-chart recorder. This will show when a potential plating problem occurs and will also describe the impedance change in detail.

- The anodes used in this program were too large for plating five pickoffs. The surface area of the anodes should be comparable to the surface area of the objects being plated. When integrated circuits are being plated (at the same current density as pickoffs), the total plating current is higher due to the greater surface area on the integrated circuits. Because anode current density is higher, a fresh and active anode surface with a low impedance is maintained. The anode size should be approximately the same surface area as the pickoffs being plated so as to increase the anode current density.
- A constant-current power supply should be used.

Any combination of these recommendations is expected to eliminate this problem. Satisfactory pickoffs have been fabricated in another program using a smaller area anode.

In the four properly electroformed lots, only two rate sensors failed to pass the component test. These sensors, Serial Number (SN) 1003 from Lot A and SN 1020 from Lot D, both had low dead-ended and flow-loaded gains. Visual inspection did not indicate any reason for the low gain: residual wax did not appear to be a problem, since these units were recleaned without any change in performance, and none of the other sensors required a second cleaning. The process had a 90-percent yield if the three improperly electroformed lots are excluded.

Rate sensor requirements are defined in Honeywell Specification DS 24949-01 (USAAMRDL-TR-76-42, Appendix B) and are summarized below:[2]

Dead-ended gain: 0.0094 ± 0.001 psid/deg/sec

Flow-loaded gain: 0.005 ± 0.001 psid/deg/sec

Flow-loaded noise: ± 1 deg/sec ≅ 0.01psid peak-to-peak

Linearity: ± 10% over ± 50 deg/sec range

Null Offset: (Left blank in Specification pending results of this program).

The rate-sensor pickoffs were evaluated using the component test station designed in Phase I of this program (see USAAMRDL-TR-75-49, Reference 1, for drawings and details). Major test station components are shown in Figure 5.

Figure 6 is a typical data sheet for a rate sensor. Table 2 gives data for all rate sensors. Rate sensor SN 1003 was rejected because of low gain (Figure 7); however, this unit would probably have operated satisfactorily in a system. Rate sensor SN 1020 had a low gain and was nonlinear, as shown in Figure 8. This sensor is a definite reject and probably has a noticeable physical internal defect; however, dissecting sensors without destroying the defect is difficult.

Four sensors have marginally acceptable gains, as shown in Table 2. Sensors 1010 and 1013 have low gains, while the gains of sensors 1006 and 1022 are high. The accepted quality control procedure is to round off the data to the same number of significant figures as the specifications requirement; i.e., three places past the decimal. Therefore, both 0.00375 and 0.00625 are within specification limits. The noise level of 0.012 psid peak-to-peak on sensor 1024 is also acceptable. Later system calibrations showed that systems with components whose performances were nearly out of specification limits were as easy to calibrate and performed as well as systems where "nominal" components were used.

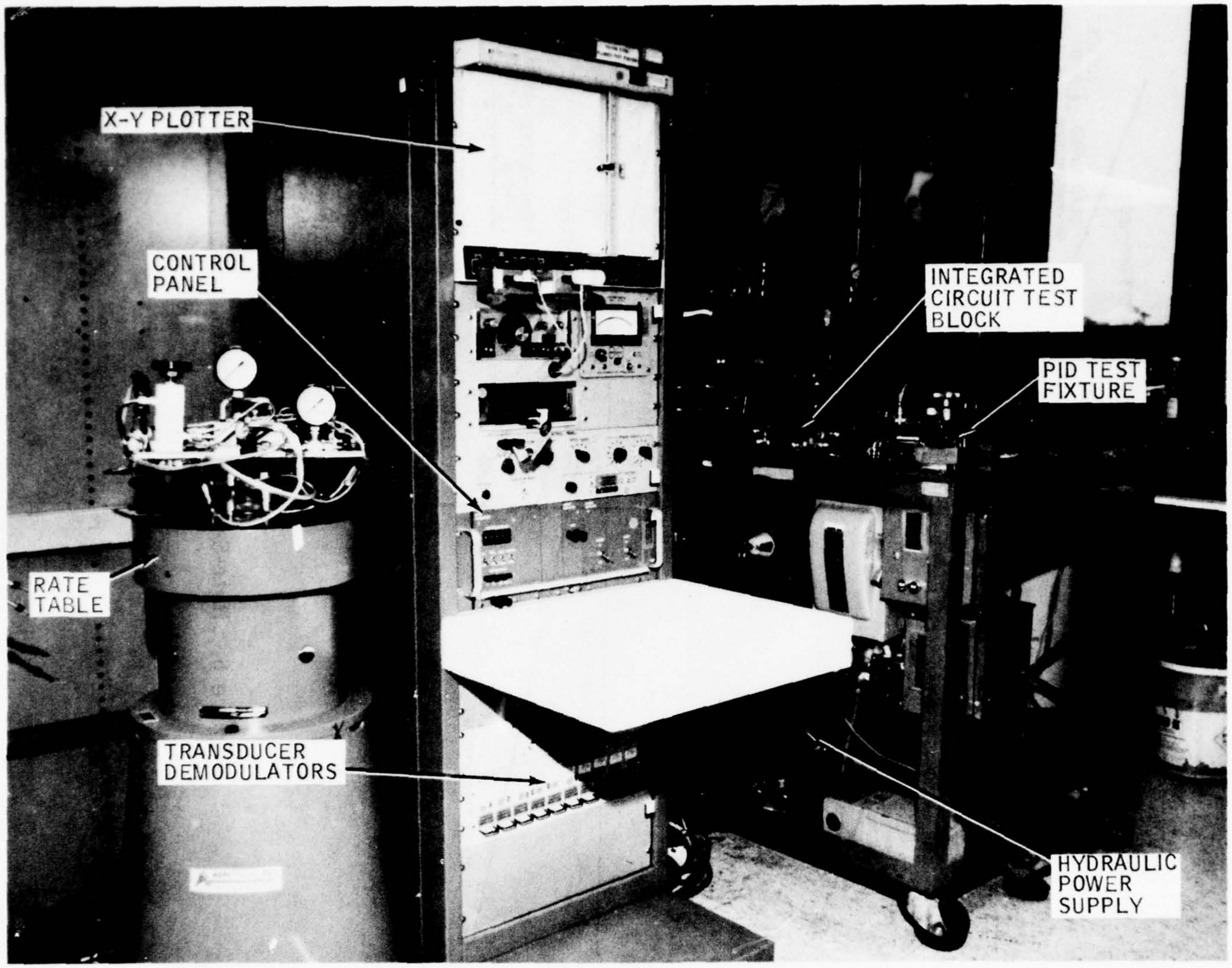

Figure 5. Component Test Station.

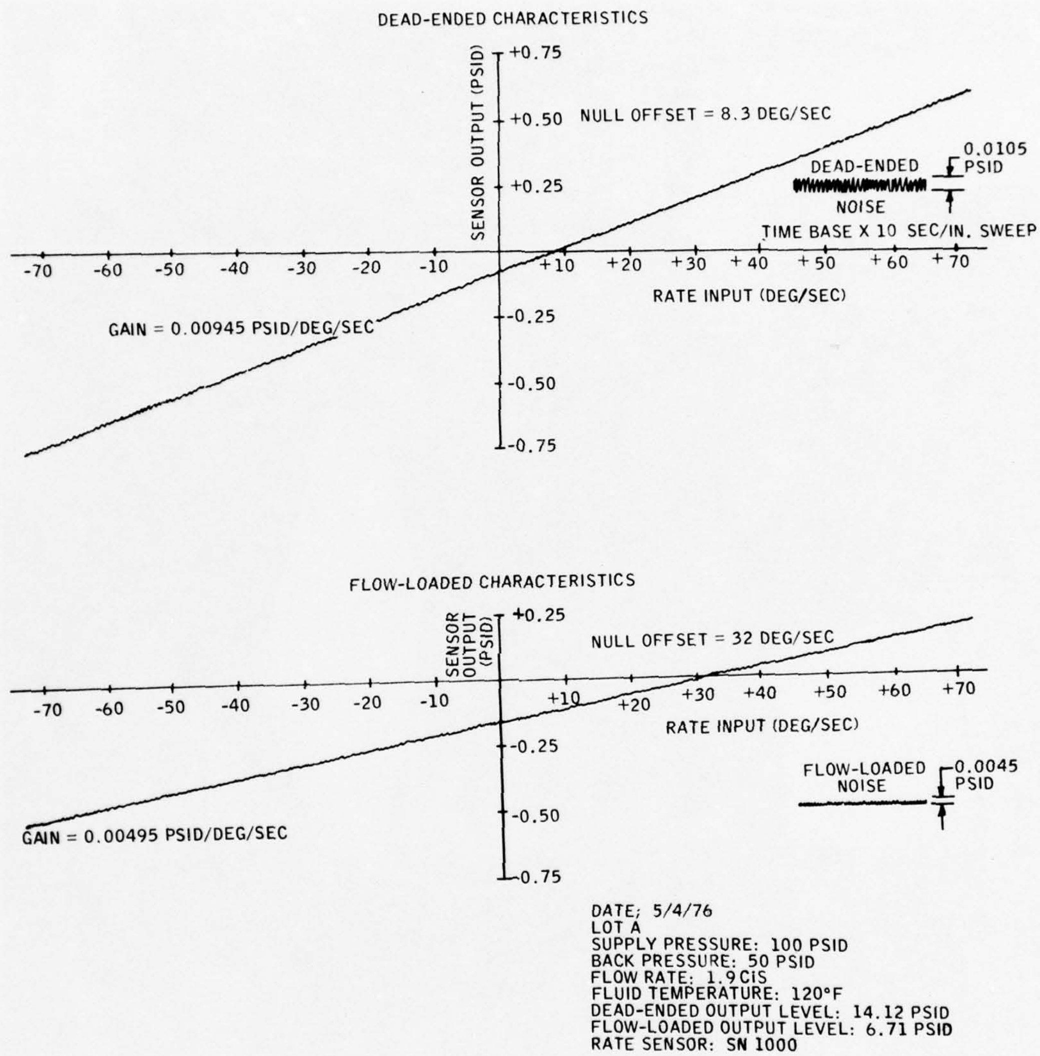

Figure 6. Rate-Sensor Test Data.

TABLE 2. RATE-SENSOR PERFORMANCE

Rate Sensor Serial Number	Dead-Ended Gain (psid/deg/sec)	Dead-Ended Offset (deg/sec)	Flow-Loaded Gain (psid/deg/sec)	Flow-Loaded Offset (psid)	Flow-Loaded Noise (psid Peak-to-Peak)	Dead-Ended Level (psid)	Flow-Loaded Level (psid)
1000	0.00945	8.3 CCW	0.00495	32.0 CCW	0.0050	14.12	6.71
1001	0.00935	13.5 CW	0.00540	10.0 CW	0.0080	14.14	6.95
1002	0.00925	32.0 CW	0.00435	7.5 CW	0.0050	14.12	6.86
1003[1]	0.00790	32.0 CW	0.00350	17.0 CW	0.0070	14.00	6.42
1004	0.00960	32.0 CW	0.00540	8.0 CW	0.0050	14.21	8.44
1005	0.00950	17.0 CW	0.00510	15.0 CCW	0.0075	14.01	6.36
1006	0.00950	18.0 CW	0.00625[2]	6.0 CW	0.0065	14.10	6.45
1007	0.00850	48.0 CW	0.00550	49.0 CW	0.0090	14.13	7.13
1008	0.00940	47.0 CW	0.00500	43.0 CW	0.0100	14.06	6.53
1009	0.00950	40.0 CW	0.00530	21.0 CW	0.0080	14.11	6.68
1010	0.00900	17.0 CW	0.00398[2]	28.0 CW	0.0095	14.11	7.35
1011	0.00920	29.0 CW	0.00515	13.0 CW	0.0080	14.16	7.08
1012	0.00940	2.0 CCW	0.00400	24.0 CW	0.0090	14.18	7.35
1013	0.00910	17.0 CW	0.00375[2]	42.0 CW	0.0100	14.19	7.55
1014	0.00960	46.0 CW	0.00470	25.0 CW	0.0080	14.16	6.88
1020[1]	0.00650					14.18	7.38
1021	0.00905	2.5 CW	0.00510	11.0 CCW	0.0080	14.14	7.04
1022	0.00970	15.0 CW	0.00620[2]	4.5 CCW	0.0090	14.11	6.51
1023	0.00820	59.0 CW	0.00455	69.5 CW	0.0100	14.15	7.47
1024	0.00925	34.0 CW	0.00515	66.0 CW	0.0120[2]	14.15	7.25
831	0.00970	23.0 CCW	0.00510	10.0 CCW	0.0045	14.15	7.14

[1] Rejected--Cause not determined. [2] Performance marginally acceptable.

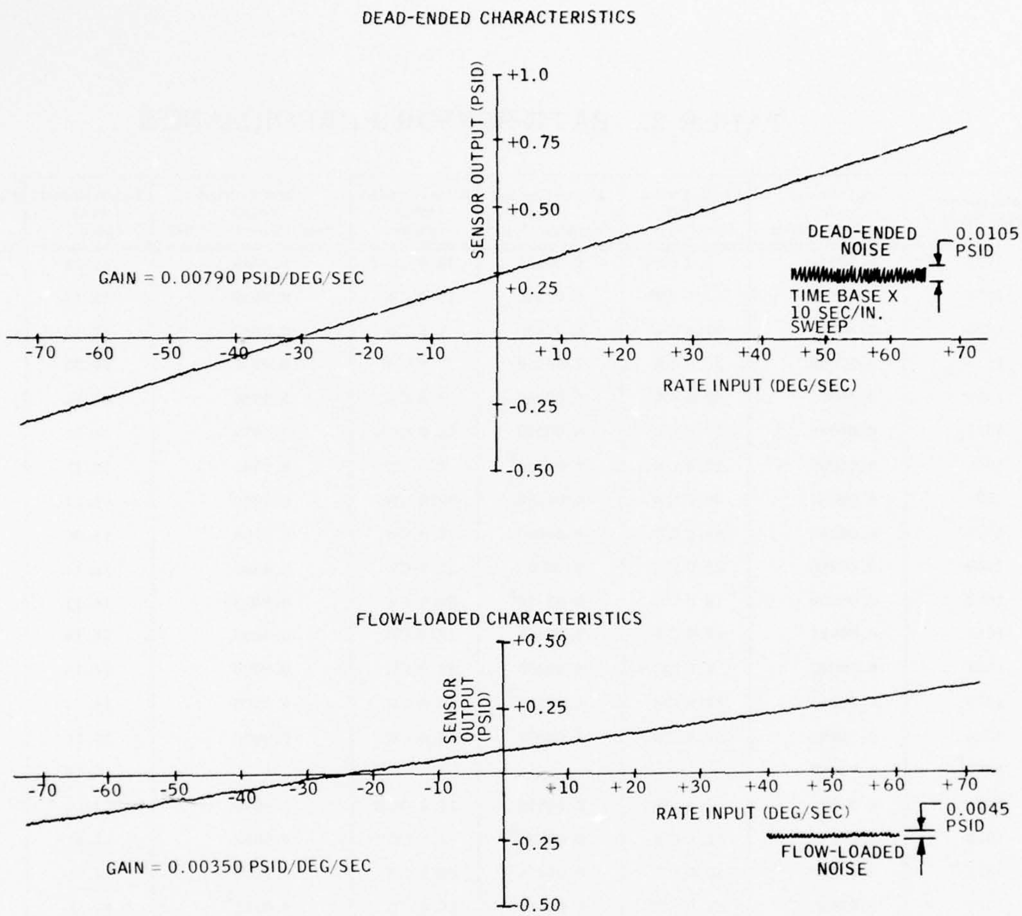

Figure 7. Rate-Sensor Serial Number 1003 Test Data.

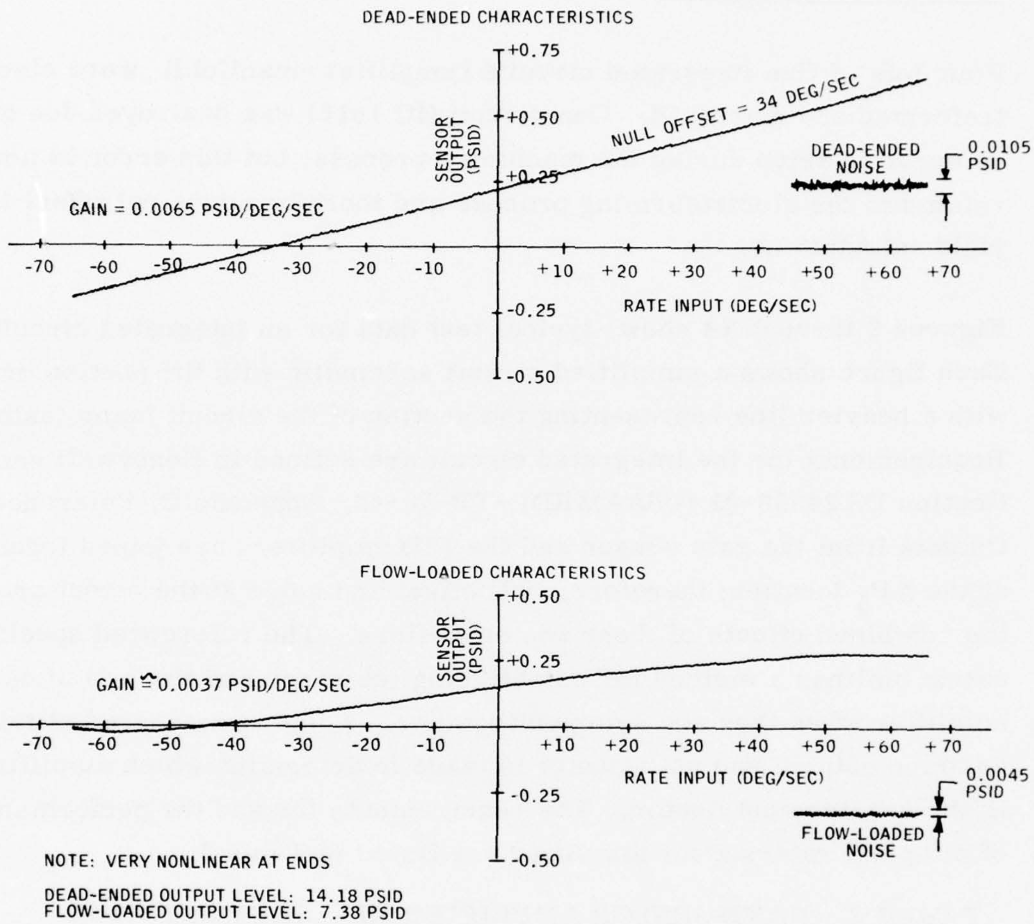

Figure 8. Rate-Sensor Serial Number 1020 Test Data.

INTEGRATED CIRCUIT

Four lots of five integrated circuits (amplifier-manifold) were electroformed and machined. One circuit (IC 1010) was destroyed due to an error in setup during the machining process, but this error is not related to the electroforming process and therefore does not affect the yield calculations.

Figures 9 through 14 show typical test data for an integrated circuit. Each figure shows a simplified circuit schematic with the portion drawn with a heavier line representing the section of the circuit being tested. Requirements for the integrated circuit are defined in Honeywell specification DS 24950-01 (USAAMRDL-TR-76-42, Appendic C, Reference 2). Outputs from the rate sensor and the PID amplifiers are joined together at the ΔP_5 location; therefore, null offset and noise at the output are the combined effects of these two amplifiers. The referenced specification outlines a method for establishing the range and the null of each amplifier when they are summed together. Noise is measured at this common output, and no attempt is made to determine which amplifier is the greater contributor. The requirements for and the performance of a typical rate-sensor amplifier are listed in Table 3.

TABLE 3. RATE-SENSOR AMPLIFIER REQUIREMENTS AND PERFORMANCE

Parameter	Requirements	Performance (SN 1008)
Gain	3.9 ± 0.5 psid/psid	4.33 psid/psid
Offset (Output)	0.5 psid max	0.25 psid
Output Linear Range	± 1 psid min	± 1.8 psid
Input Range before Reversal	± 0.5 psid min	± 0.7 psid
Noise	0.03 psid peak-to-peak	0.01 psid peak-to-peak
Linearity	± 0.15 psid (over +1 psid range)	- 0.06 psid

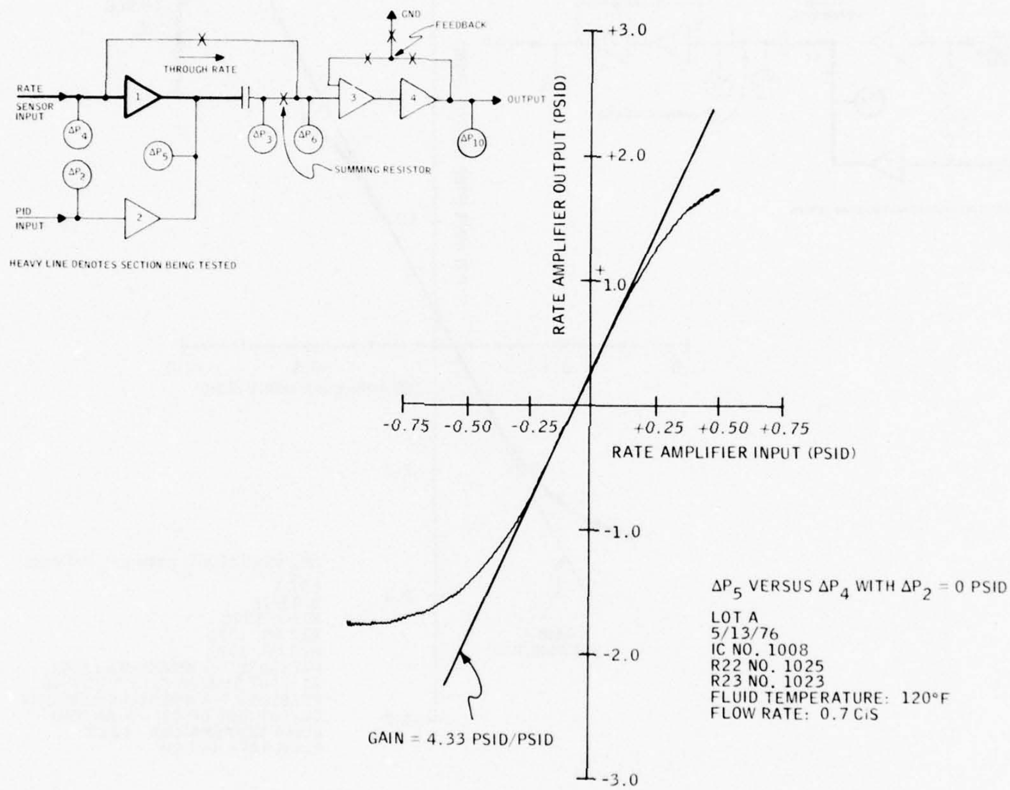

Figure 9. Rate-Sensor Amplifier Performance.

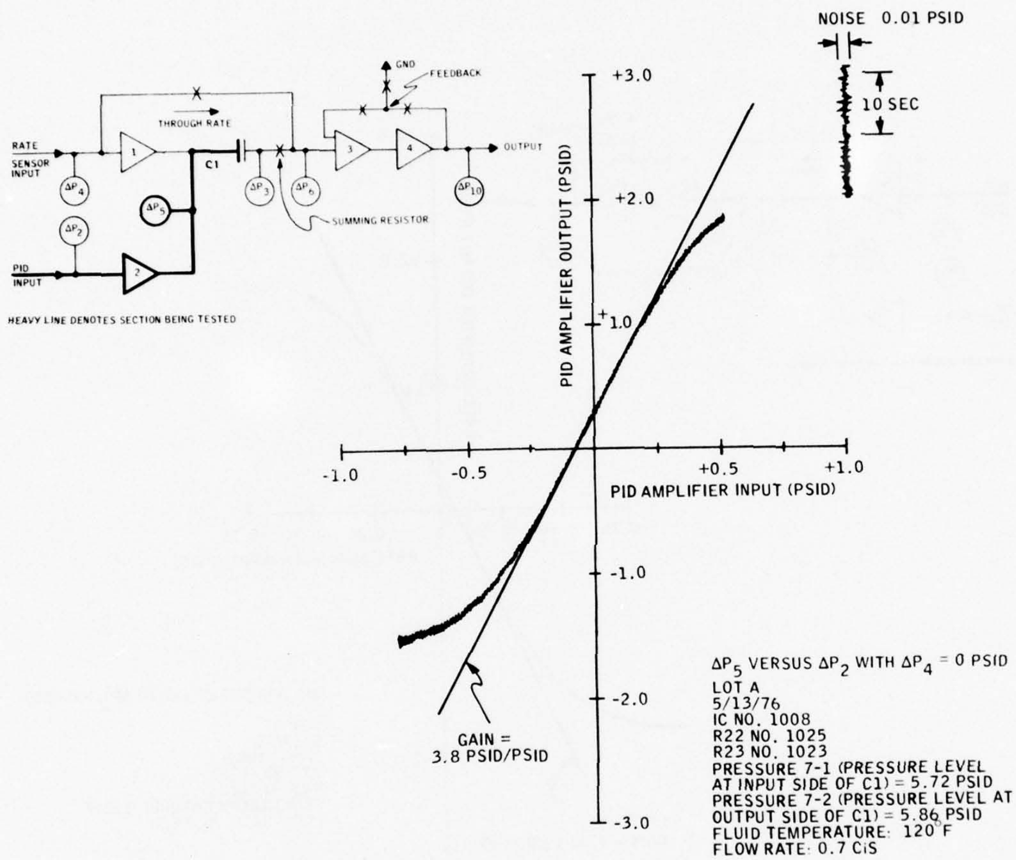

Figure 10. PID Amplifier Performance.

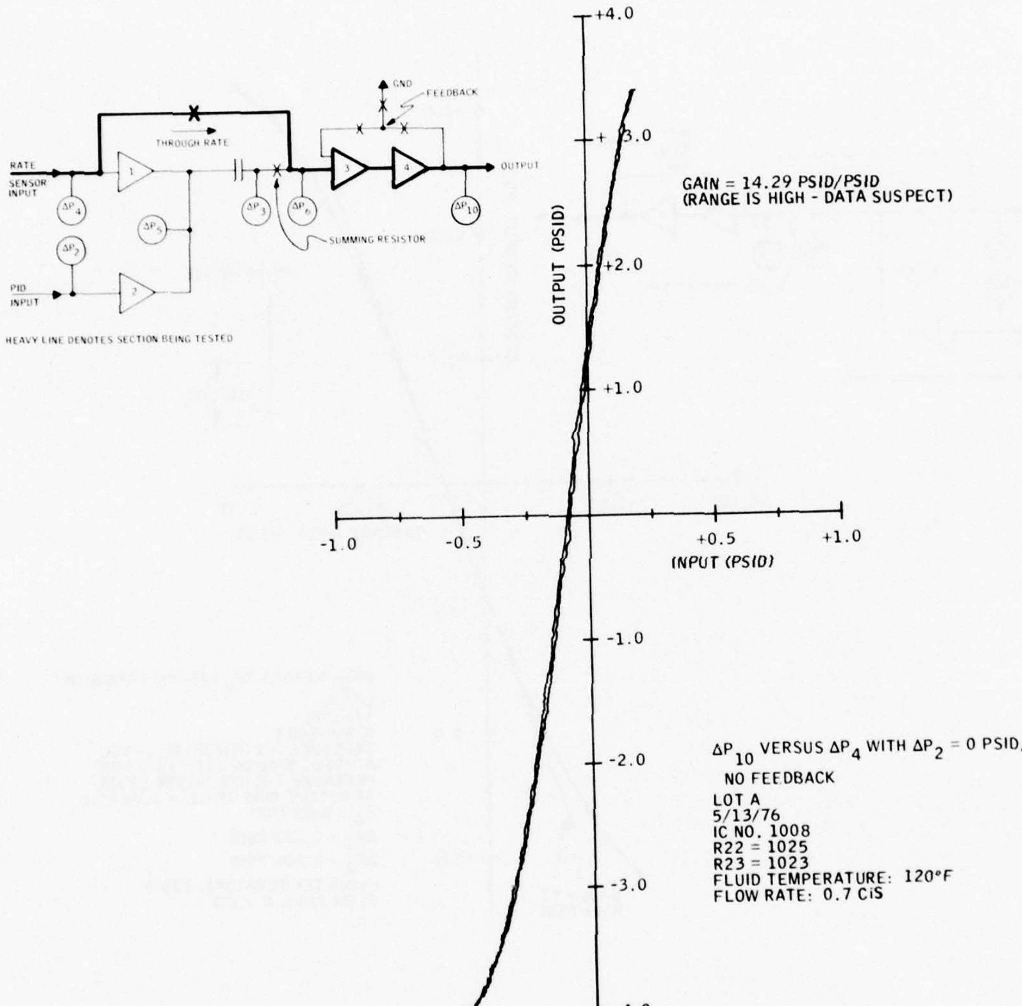

Figure 11. Through-Rate Gain.

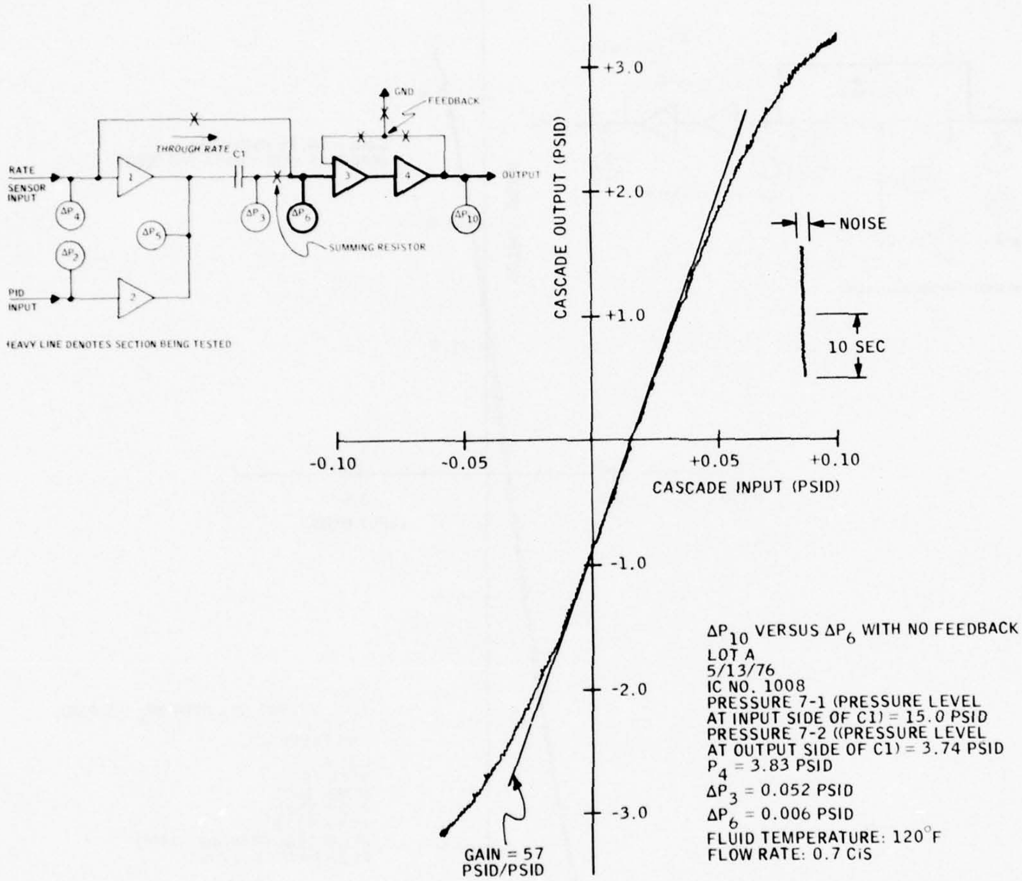

Figure 12. Output Cascade Characteristics.

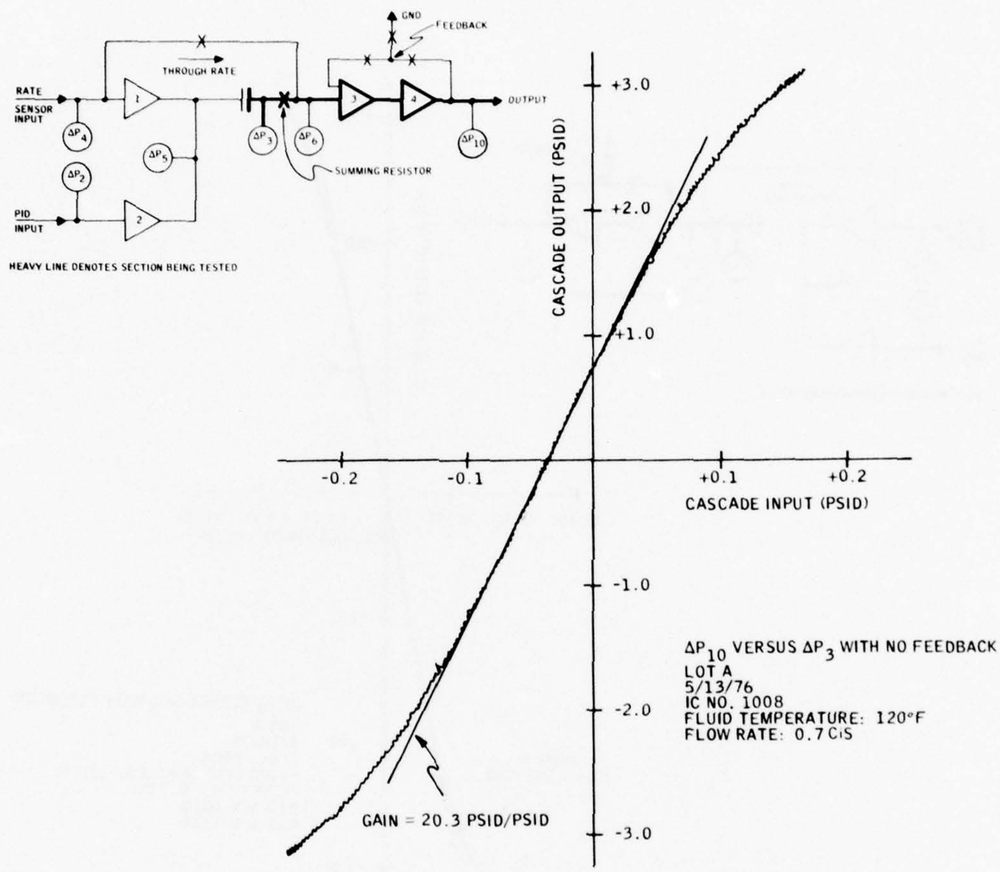

Figure 13. Output Cascade and Input Resistor Characteristics.

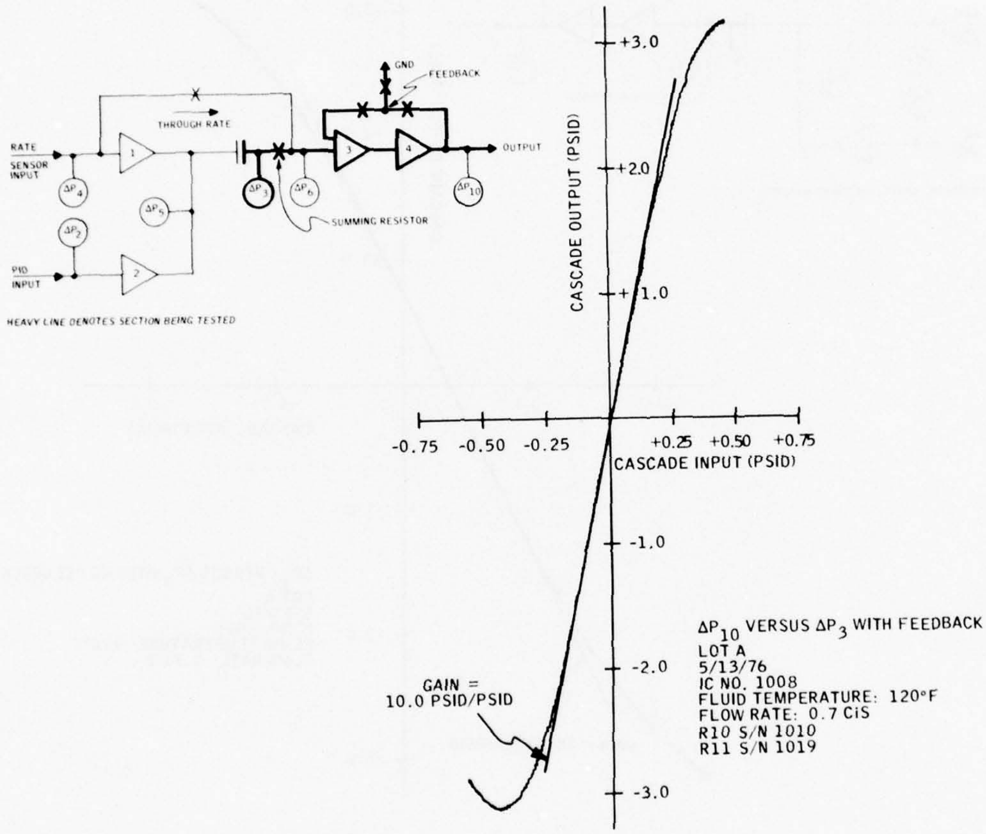

Figure 14. Output Cascade with Feedback.

The gain of the nominal rate-sensor amplifier, shown in Figure 9, is somewhat higher than anticipated. However, resistors R6 and R7, shown in the Figure 2 schematic, can reduce effective gain to compensate for a high gain in the rate-sensor amplifier. Results of this program indicate that the specification gain requirements should be changed to 4.3 ± 0.6 psid/psid. Offset, range, and noise were recorded and tabulated for all rate-sensor amplifiers, and are shown in Table 4. Range and linearity were all well within specification limits and were not calculated or tabulated for most circuits.

PID amplifier requirements are identical to those of the rate-sensor amplifier except that the gain is specified to be 3.6 ± 0.5 psid/psid. Figure 10 gives the test results.

Through-rate gain measurements (as shown in Figure 11) are a test of the electroformed through-rate resistors (R22 and R23, Figure 7), as well as the output cascade. This data would be somewhat more significant if the output amplifier cascade were operating with normal feedback. The specification requirement should be changed to 7 ± 1.0 psid/psid for through-rate gain with feedback. Any problem with the output cascade bias resistors, feedback resistors, or through-rate resistors would show up in this single test. Present specification requirements for testing are much more complex than those required to eliminate unsatisfactory units. However, the additional data obtained in this program showed the statistical variations of numerous characteristics throughout the circuit and helped to isolate problem areas.

Output cascade characteristics are shown in Figure 12. The calculated gain of 57 psid/psid compares favorably with the specification requirements of 54 ± 11 psid/psid. Offset is 0.016 psid at the input, which is well within specification limits.

TABLE 4. INTEGRATED CIRCUIT PERFORMANCE SUMMARY

1	2	3	4	5	6	7	8	9	10	11	12	13	14	15	16	17
Integrated Circuit Serial Number	Date Tested	Circuit Pressure Drop (psid)	Rate Amplifier Gain (psid/psid)	Rate Amplifier Null Output (psid)	Rate Amplifier and PID Amplifier Noise (psid, Peak-to-Peak)	PID Amplifier Gain (psid/psid)	PID Amplifier Output Offset (psid)	Through-Rate Gain (psid/psid)	Through-Rate Null at ΔP_4 (psid)	Output Cascade Gain (psid/psid)	Output Cascade Null at Input (psid)	Output Cascade Noise (psid, Peak-to-Peak)	Output Cascade Gain with Input Resistors (psid/psid)	Output Cascade Gain with Feedback (psid/psid)	Level 7-1 Into High-Pass Capacitor C_1 (psid above Return)	Level 7-1 Out of High-Pass Capacitor C_1 (psid above Return)
1000	5-11	16.05	4.50	+0.30	0.005	3.33	+0.10	15.38	-0.145	55.90	+0.021	0.015	19.59	10.00	5.87	5.87
1001	5-19	14.40	(Rejected for nonlinear output - see text)													
1002	5-12	14.90	4.44	+0.25	0.012	3.26	-0.25	14.13	-0.138	54.54	+0.012	0.050	21.18	10.04	5.45	5.36
1003	5-12	15.05	4.67	+0.65	0.028	3.37	-0.25	12.00	-0.185	47.14	+0.030	0.035	17.41	9.68	5.86	5.88
1004	5-12	15.65	4.38	+0.30	0.020	3.57	-0.10	10.70	-0.025	47.50	+0.010	0.003	17.74	9.75	5.92	5.95
1005	5-17	14.60	4.35	+0.40	0.014	2.98	+0.05	14.29	-0.132	58.06	+0.008	0.014	20.50	10.20	*	*
1006	5-18	14.80	4.19	+0.20	0.011	3.16	+0.05	14.08	-0.108	59.17	+0.018	0.014	20.80	10.10	5.84	5.87
1007	5-19	17.50	4.50	+0.35	0.012	2.99	-0.20	13.89	-0.030	31.31	-0.003	0.033	15.99	8.97	5.73	5.67
1008	5-13	15.00	4.33	+0.25	0.010	3.80	+0.10	14.29	-0.088	57.05	+0.016	0.003	20.34	10.00	5.72	5.86
1009	5-17	14.45	4.21	+0.25	0.019	3.36	-0.30	13.51	-0.183	53.33	+0.011	0.041	19.52	9.76	*	*
1010	(Not tested - destroyed during machining)															
1011	6-22	15.90	4.14	+0.30	0.026	3.24	-0.20	11.63	-0.200	52.63	+0.004	0.018	19.07	9.90	5.74	5.59
1012	6-22	15.50	4.13	+0.15	0.005	3.38	+0.15	13.80	-0.180	54.94	+0.016	*	20.75	10.36	5.72	5.76
1013	6-22	15.00	4.38	+0.30	0.019	3.55	0	13.17	-0.270	53.61	0	0.014	19.72	9.66	5.79	5.74
1014	6-22	15.25	4.42	+0.10	0.025	3.24	-0.05	14.29	-0.115	56.70	+0.009	0.016	18.59	10.53	5.90	5.87
1015	6-23	16.55	4.09	+0.20	0.052	3.52	+0.25	14.93	-0.058	54.49	+0.019	0.012	20.49	10.00	5.89	6.01
1016	6-23	20.80	(Rejected - no power to one stage of output cascade)							1.30						
1017	6-22	15.75	4.24	+0.10	0.009	3.05	+0.30	12.05	-0.188	52.63	+0.010	*	20.83	10.47	5.76	5.79
1018	6-22	16.55	4.03	+0.30	*	3.38	+0.10	15.15	-0.245	51.68	+0.030	*	20.00	9.80	5.83	5.82
1019	6-23	16.15	4.38	+0.35	0.007	3.06	+0.10	15.15	-0.290	54.05	-0.028	*	20.20	10.31	5.94	5.81
851	5-19	15.25	4.43	+0.30	0.019	3.39	+0.10	14.92	-0.243	50.00	+0.010	0.030	19.31	10.10	*	*
853	6-21	15.25	4.27	+0.40	0.010	3.14	-0.15	13.16	-0.090	53.19	+0.020	0.003	19.57	9.71	*	*

* Data not available

The Figure 13 data shows that the summing resistors have a gain of about 0.36 psid/psid and can have a slight effect on cascade null. Feedback reduces the gain and improves the null as shown in Figure 14.

The integrated circuit performances of all units fabricated are shown in Table 4. Circuit differential pressure (column three) is relatively constant, although it is high for IC SN 1007 and IC SN 1016. Gain of the output cascade is low on IC 1007; however, the performance of its rate and PID amplifiers is consistent with that of other circuits. Circuit 1007, which could have been rejected because of its slightly low gain, proved to be satisfactory when calibrated in a system. Circuit 1016 had the highest circuit differential pressure, and test results showed that its output cascade had a very low gain and a small output range. The output range was only ±0.25 psid, as compared to about ±3 psid for a normal amplifier, indicating that one or more of the output amplifier stages had its power supply blocked. This blockage would result in more flow to the PID amplifier and would show up as higher than normal gain and range. Tests proved this to be the case.

Rate amplifier characteristics (columns 4 through 6) show that gain is constant within about ± 8 percent. Null offset is always in the same direction, indicating some basic offset in the mold. Null on IC 1003 was slightly above specification requirements; however, it was accepted pending systems calibration results.

PID amplifier data (columns 7 and 8) show that gain varies by about ±12 percent. Null is well within specification limits and varies in both directions, indicating very little offset in the PID amplifier mold. Through-rate characteristics are shown in Columns 9 and 10. IC 1004 has the lowest gain, 10.7 psid/psid, which is somewhat less than would be expected based on the performance of the output cascade. Part of the inconsistency is due to a data acquisition error. Gain is

determined graphically (see Figure 12) by drawing a "best straight line" through the gain curve and by counting squares to determine its slope. It would be desirable to expand the input scale by a factor of 2 or 2.5 to reduce this slope; however, the specific X-Y plotter used in this program could only expand it by a factor of five, which would have resulted in a loss of data at the ends of the curve.

The variation in this parameter indicated a very acceptable ±18-percent linearity, even with this data acquisition limitation. Null offset is somewhat larger than anticipated, but there were no indications that this offset caused any calibration problems. Both gain and null offset readings on through-rate measurement would be more significant if the output amplifier were operating with feedback (as previously discussed).

Open-loop characteristics of the two-stage output cascade are tabulated in columns 11 through 13 of Table 4. With the exception of integrated circuit 1007, the gain is very consistent (±10%). Errors tend to compound in a two-stage cascade; however, this cascade gain only varies approximately the same percentage as the single-stage rate-sensor amplifier or PID amplifier. Output cascade null remained well within limits, and noise was about one order of magnitude less than that allowed in the specification.

The output cascade on rejected circuit SN 1001 had a gain that is slightly low and nonlinear, as shown in Figure 15. Interaction regions of the output cascade were removed, and the receiver section was inspected. The output amplifier had a curtain caused by a crack in the wax mandrel. The location of this curtain is shown in Figure 15.

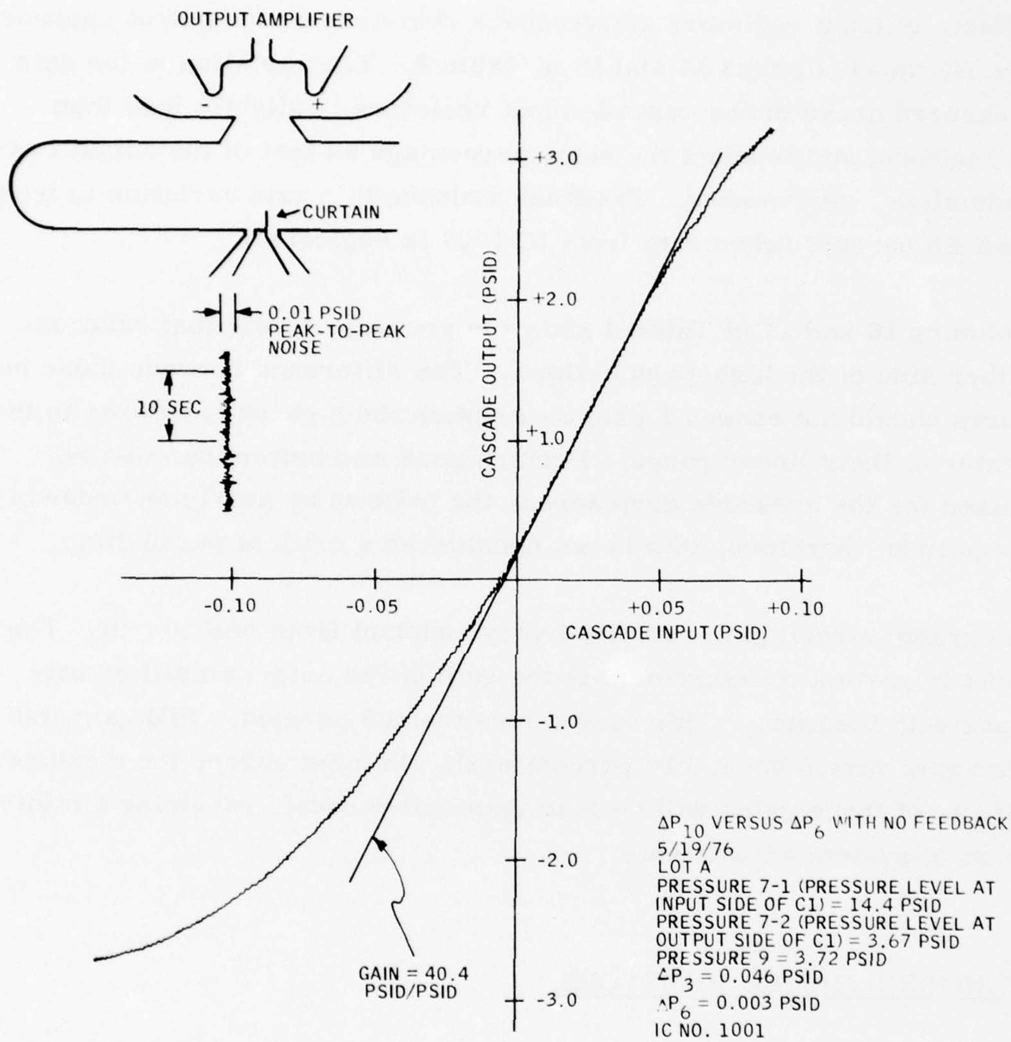

Figure 15. Nonlinear Output Cascade.

Effects of input resistors and feedback resistors on the output cascade are shown in columns 14 and 15 of Table 4. The variation in the gain measured ahead of the cascade input resistors is slightly less than ±10 percent and is about the same percentage as that of the output cascade alone, as expected. Feedback reduces this gain variation to less than ± 5 percent (when data from IC 1007 is neglected).

Columns 16 and 17 of Table 4 show the pressure levels that exist on either side of the high-pass bellows. The difference between these pressures should not exceed 1 psid to maintain the high-pass bellows in the center of their linear range. Performance was better than that required for the pressure drop across the bellows by nearly an order of magnitude; therefore, this is not considered a critical parameter.

Integrated circuit gain remained very constant from unit to unit. The most important measurement is the gain of the output amplifier network with feedback. This varied less than ± 5 percent. PID gain and rate gain varied about ± 10 percent each. In most cases, the combined effects of these gains will be less than ± 10 percent, requiring a minimum of system adjustments.

ELECTROFORMED RESISTORS

Ten electroformed resistors are shown in the Figure 2 schematic. Resistors R27a, R28a, R29, R30, and R31 are all electroformed into the integrated circuit. Testing showed that the R27a and the R28a are excellently matched. Bolt-on feedback resistors R10 and R11 were tested on the integrated circuit by operating the output cascade with and without feedback. Feedback reduced the gain by a factor of two and the gain variation from about ± 10 percent to less than ± 5 percent. The

exceptional performance of the output cascade with the feedback resistors indicates that they are accurate to ±5 percent. This degree of accuracy is excellent when each electroformed feedback resistor block contains eleven resistor elements. Through-rate gain measurements indicate that resistor elements R22 and R23 are relatively consistent. Experience in this program indicates that the electroformed resistors are more consistent (accurate and repeatable) than the resistors with the drilled or punched orifices used in other parts of the circuit.

PID VALVE DATA

PID valves are nonelectroformed components and, therefore, were fabricated in a single lot rather than in four separate lots. However, PID valves were tested in lots after they were mounted in the housings.

Gain and linearity are the only significant parameters defined in Honeywell specification DS 25515-01 (USAAMRDL-TR-76-42, Appendix A). As specified, the gain should be 7.8 ± 1.2 psid/inch of spool travel. Linearity, defined as the maximum deviation from the nominal gain curve over the ±0.04-inch operating range, is required to be better than ± 0.06 psid. Figure 16 is a typical gain curve. This unit is satisfactory, since the maximum deviation is only 0.045 psid at 0.04 inch stroke, which is less than the tolerable 0.06 psid. The gain of 6.71 psid/inch is only slightly higher than the minimum limit of 6.6 psid/inch. PID data for all controllers is summarized in Table 5.

Thirty-one valves were tested to obtain twenty satisfactory controllers for a 65-percent yield. Inspection of the rejected units showed that some had slight steps in their sleeve bores and all had poor surface finishes in this area. Drawings were modified to require a 16 microfinish in this critical area, and yield should be greatly improved in

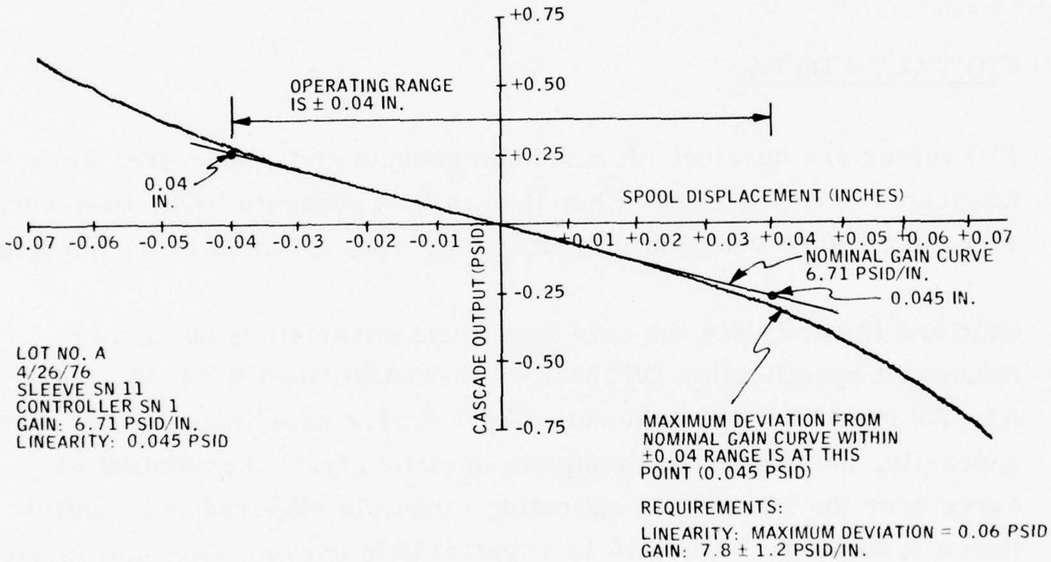

Figure 16. PID Gain Curve.

TABLE 5. PID PERFORMANCE SUMMARY

Controller SN	Sleeve SN	Gain psid/in.	Linearity psid	Comments
1	X	6.750	0.113	Rejected. Step in sleeve I.D.
1	11	6.710	0.045	
2	20	6.250	0.220	Rejected. Poor linearity.
2	21	5.370	0.043	Rejected. Low gain, poor inside finish.
2	19	9.200	0.055	
3	1	7.370	0.015	
4	28	8.060	0.045	
5	18	6.250	0.087	Rejected. Poor gain and linearity.
5	30	8.960	0.052	
6	3	7.030	0.055	
7	15	7.656	0.025	
8	27	8.060	0.032	
9	37	6.875	0.040	
10	2	6.090	0.020	Rejected. Low gain.
10	33	8.375	0.030	
11	32	6.880	0.050	
12	23	8.740	0.075	
13	13	8.120	0.100	Rejected. Linearity.
13	22	8.070	0.075	
14	34	6.250	0.035	Rejected. Low gain.
14	39	7.750	0.075	

TABLE 5. PID PERFORMANCE SUMMARY
(CONCLUDED)

Controller SN	Sleeve SN	Gain psid/in.	Linearity psid	Comments
15	8	10.00	0.075	Rejected. High gain.
15	38	7.40	0.050	
16	26	8.44	0.050	
17	6	8.13	0.062	
18	14	7.50	0.075	
19	41	6.25	0.050	Rejected. Low gain.
19	40	6.41	0.026	Rejected. Low gain.
19	31	6.20	0.100	Rejected. Low gain.
19	43	8.59	0.050	
20	36	7.59	0.068	

any future production run. PID gain varied from unit to unit by ±15 percent even after rejecting 35 percent of the units tested. This variation was the greatest variation of all components in the system.

FLOW-CONTROL VALVE

Commercially available flow-control valves were used in this system, and they were calibrated to minimize the difference in flow between one system and another. Figure 17 is a sketch of the flow-control valve. Flow-control valve output can be increased by adding more preload to the spring. Each 0.020-thick washer would add sufficient preload to increase flow by about 0.014 gpm. This method proved to be more satisfactory than attempting to increase metering orifice area. Flow-control valve calibration data is given in Table 6. A sufficient number of valves were available to permit selecting only those with a flow of 0.7 gpm ± 1 percent. This rigid control of system flow reduced the number of variables and permitted a more accurate evaluation of the electroformed components. A ±1-percent flow valve is recommended for future systems to minimize system calibration requirements and to improve the interchangeability of the systems.

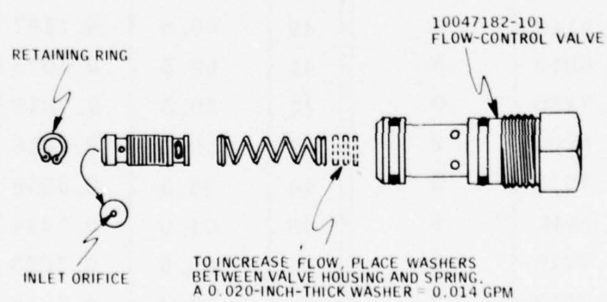

Figure 17. Flow-Control Valve.

TABLE 6. FLOW-CONTROL VALVE CALIBRATION DATA

Fluid Temperature: 120 ± 5°F
Spacer Size: 0.015 in.
Pressure Across Valve: 400 psid

SN	Meter Reading	Flow (GPM)	Quantity of Spacers	SN	Meter Reading	Flow (GPM)	Quantity of Spacers
1	60.5	0.7187	0	25	59.5	0.7073	0
2	61.0	0.7244	Drilled Orifice Larger	26	65.5	0.7784	0
				27	62.5	0.7427	0
				28	59.0	0.7016	0
3	60.5	0.7187	Drilled Orifice Larger	29	68.5	0.8140	0
				30	58.5	0.6958	5
4	Damaged			31	58.0	0.6901	1
5	58.0	0.6901	6	32	67.0	0.7962	0
6	Damaged			33	59.5	0.7073	2
7	59.0	0.7016	0				
8	62.0	0.7368	0	34	59.0	0.7016	1 Spacer Drilled Orifice
9	60.5	0.7187	0				
10	65.0	0.7724	0				
11	59.0	0.7016	4	35	59.0	0.7016	4
12	58.5	0.6958	0	36	59.0	0.7016	1
13	60.5	0.7187	0	37	59.0	0.7016	3
14	61.0	0.7244	0	38	58.0	0.6901	0
15	59.0	0.7016	4	39	59.0	0.7016	0
16	68.5	0.8140	0	40	60.5	0.7187	0
17	58.5	0.6958	6	41	59.5	0.7073	0
18	60.0	0.7130	0	42	59.0	0.7016	4
19	58.0	0.6901	2	43	59.0	0.7016	0
20	59.0	0.7016	2	44	58.5	0.6958	5
21	63.5	0.7546	0	45	61.0	0.7244	0
22	59.0	0.7016	5	46	59.5	0.7073	5
23	59.5	0.7073	0	47	59.0	0.7016	0
24	60.0	0.7130	0	48	59.0	0.7016	3
				49	58.5	0.6958	3

SECTION IV
SENSOR/CONTROLLER ASSEMBLY AND CALIBRATION

SENSOR/CONTROLLER ASSEMBLY

Each lot of components was tested, and then the components were randomly assembled into systems. During the assembly of Lot A, the rejected rate sensor and rejected integrated circuit were replaced with components from Lot B. The missing components in Lot B were replaced with components from Phase II. Table 7 lists the components used in the assembled systems. Note that four of the bolt-on resistors in Lot B are in the 800 series from Phase II of this program: the original resistors were temporarily misplaced in the cleaning process.

Systems were proof pressure tested to 900 psid for one minute before and after calibration. Three through-rate resistors, R23, failed during these tests. Two failures occurred on controller 9 and one occurred on controller 6. A minor redesign would eliminate the sharp corners, reducing the stress concentration and resulting in increased plating thickness in the critical areas.

The failed resistors were SN 840, 1037, and 1041. Two of these were fabricated in Phase III. Thirty-six out of 38, or 94.7 percent, of through-rate resistors were satisfactory, and 35 out of 35, or 100 percent, of tested feedback resistors were satisfactory. Overall yield for bolt-on resistors was 71 out of 73, or 97.3 percent.

Integrated circuit SN 853 on system 11 developed a slight leak during proof pressure tests. This circuit was soldered, retested, and then calibrated without further problems. This is not taken into account in yield calculations because the circuit was from Phase II and because it

TABLE 7. CONFIGURATION OF ASSEMBLED SYSTEMS

Lot	System	PID Sleeve	Integrated Circuit	Rate Sensor	Flow Control	Resistor R10	Resistor R11	Resistor R22	Resistor R23
A	1	11	1008	1001	39	1010	1019	1025	1023
	2	19	1003	1002	46	1012	1013	1027	1028
	3	1	1000	1009	35	1018	1014	1024	1021
	4	28	1004	1004	20	1015	1011	1028A	1022
	5	30	1002	1000	41	1016	1017	1020	1026
B	6	3	1006	1006	34	1034	1035	1036	1037[a]
	7	15	1009	1005	23	1030	1031	1032	1033
	8	27	1007	1008	43	1038	844	1930	835
	9	37	851	831	15	842	845	1040	1041[b]
	10	33	1005	1007	36	1027A	1026A	1028B	1029
C	11	32	853	1010	7	1043	1042	1060	1059
	12	23	1012	1011	11	1049	1046	1056	1061
	13	22	1013	1012	22	1051	1045	1053	1054
	14	39	1014	1013	28	1047	1048	1055	1057
	15	38	1011	1014	42	1044	1050	1052	1058
D	16	26	1015	1021	17	1070	1071	1072	1073
	17	6	1017	1022	37	1066	1064	1078	1080
	18	14	1018	1023	44	1069	1068	1076	1077
	19	43	1019	1024	12	1063	1062	1074	1075
	20	36	This system was not assembled.						

[a]Replaced with 1079.

[b]Replaced with 840 then 837.

was repaired. The failed electroformed resistors could also have been repaired if they were needed. Phase II components were repaired and/ or used only to obtain the maximum number of system assemblies, since no other provisions for "scrap" were made in this program.

None of the failures or leaks in the integrated circuits were related to bonding problems. The revised plating process developed on Phase II produced 120 components without any indication of marginal adhesion.

Another assembly problem occurred involving capacitor C1 in controller SN 2. Null offset changes were traced to this capacitor; the input signal ports were partially blocked by part of the capacitor (Figure 18). Clearance "C" in this figure was less than 0.005 inch because of a stackup of tolerances and because the grooves in the covers were slightly too deep. Clearance "C" was shimmed to 0.020 inch during the soldering process. This step was not included in the production process detail submitted earlier in this program and will not be necessary if capacitor covers are machined within specified tolerances. It is recommended that drawing No. 10050026 be modified to require a minimum clearance of 0.015 inch to ensure that this dimension will be inspected.

Final assembly inspection showed that the mounting hole locations exceeded YG1158 drawing tolerances on some controllers. The mounting hangar and mounting bar were shifted slightly to locate these holes properly. Signal ports in the outlet block were off of nominal by nearly 0.030 inch (all controllers were out of limits). These controllers were satisfactory for the test fixture used on this program, but the outlet block should be modified if they are to be used with the Hydraulic Research Model 30005000 servoactuator. Honeywell drawings 10050022 (manifold, amplifier) and 10050024 (block, outlet) were revised to provide the required nominal port location. It will be necessary to modify

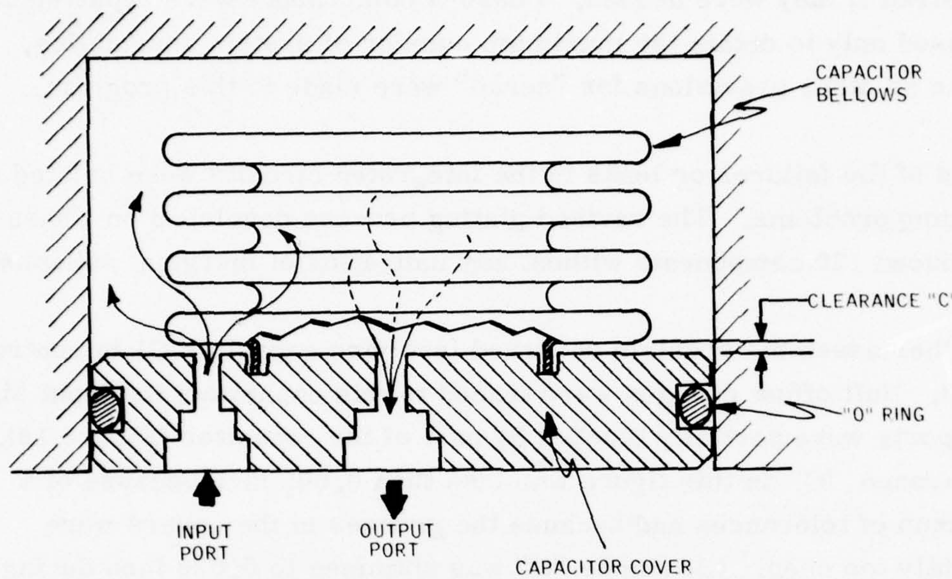

Figure 18. Blocked Capacitor.

the production process detail on the amplifier manifold, 10050022-11, to be compatible with the revised machining process defined in the drawing. The revised machining process is more accurate in controlling the effective thickness of this manifold (integrated circuit) to minimize the stackup of tolerances on the outlet block port locations.

The yields of the electroform process are summarized in Table 8. These calculations do not include the integrated circuit that was improperly machined or the three rejected lots of rate-sensor pickoffs. Because it was necessary to change the process to get satisfactory sensors, the "official" start of pickoff electroforming occurred after the two lots were rejected. The third lot of unsatisfactory pickoffs, which was rejected before machining, was also not included in the yield calculations. If this lot were included, the overall yield would be reduced from 94.6 percent to 90.6 percent. Proper control of the plating current should eliminate the pickoff problem, although it is

TABLE 8. COMPONENT YIELD SUMMARY

Component	Number Fabricated and Tested	Number Satisfactory	Yield (Percent)
Electroformed Components			
Rate Sensor	20	18	90.0
Integrated Circuit	19	17	89.5
Through-rate Resistors	38	36	94.7
Feedback Resistors	35	35	100.0
Total	112	106	94.6
Nonelectroformed Components			
Lag Capacitors	19	19	100.0
High-pass Capacitors	39	38	97.4
Housings	19	19	100.0
PID Valves	31	20	64.5

estimated that random rejections will occur throughout production. Yield is expected to remain at about 95 percent until a representative group of rejects is analyzed and process modifications are incorporated.

The yields of several nonelectroformed components are also given in Table 8. This data confirms the need for improved PID valve performance. A revised PID sleeve drawing that specifies interior surface finishes should improve the yield to 90 percent or better.

SENSOR/CONTROLLER CALIBRATION

After assembly, all controllers were calibrated at a fluid temperature of 120°F. The modifications or adjustments required to obtain the specified responses were recorded on a calibration data sheet for each controller. Complete frequency response data was obtained for both rate input and PID input. Table 9 lists the hardware adjustments and changes. Nearly one-third of the systems met system requirements without any adjustments. The significance of the adjustments made can be understood by observing the resistor locations in Figure 2. R27b and R28b are in series with the 0.015 x 0.015-inch electroformed bias restrictors. Note that these orifices, which are used to null system output, have a much larger area than the electroformed resistors and have only small effects on the differential pressures ahead of R8 and R9. The smallest orifice has the greatest effect, about 0.15 psid at this bias location.

The addition of orifices in leg "c" of feedback resistors R10 and R11 increased the amount of feedback and therefore reduced the output cascade gain. The greatest gain reduction was applied to controller SN 8, where the 0.018-inch-diameter resistors reduced the gain about 40 percent. Resistors in leg "a" or leg "b" of feedback resistors R10 and R11 reduced the amount of feedback and therefore increased output amplifier gain. Gain was increased by about 15 percent when a matched pair of 0.011-inch-diameter resistors were placed in the two "a" locations. Resistors 6 and 7 at the output of amplifier A_I reduced the system rate gain without reducing PID gain, and removing these resistors increased rate gain by about 15 percent. Resistor pair R14 and R15 tended to reduce PID gain slightly and increase the effective output impedance of the PID valve. Reducing their sizes from 0.026 inch, in the case of controller 5, or removing them entirely, as in the case of controller 18, had an effect of about ±20 percent. An 0.085-inch-thick PID

TABLE 9. REQUIRED CHANGES FOR CALIBRATION

Controller	R27b (in.)	R28b (in.)	Series R10, 11c (in.)	Series R10, 11b (in.)	Series R10, 11a	R6, 7	R14, 15	PID Plate Shim (in.)	Sensor Bias Orifice (in.)	Miscellaneous
1	S	0.020	S	S	S	S	S	0.073	None	
2	0.024	S	S	0.018	0.011	S	S	0.064	0.023 (Left Side)	
3	S	0.024	S	0.011	S	S	0.024	None	None	
4	S	0.020	S	S	S	Removed	S	0.042	None	
5	S	S	S	S	S	S	0.020	None	None	
6	S	0.022	0.026	S	S	S	S	None	None	
7	S	S	S	S	S	S	S	None	None	
8	S	0.022	0.018	S	S	S	S	0.064	None	+ one coupling element
9	S	S	S	S	S	S	S	0.064	None	
10	S	0.020	0.020	S	S	S	S	0.064	None	
11	S	0.022	S	S	S	S	S	None	None	
12	S	S	S	S	S	S	S	None	None	
13	0.026	S	S	S	S	S	S	0.085	None	
14	S	S	S	S	S	S	S	None	None	
15	0.025	S	S	0.011	S	S	S	None	0.028 (Left Side)	
16	S	S	S	S	S	S	S	None	None	
17	S	S	S	S	S	S	S	None	None	
18	S	S	S	S	S	S	Open	None	None	
19	S	S	S	S	S	S	S	None	None	

S = standard per Figure 2.

plate shim increased PID gain about 50 percent. It was necessary to add bias restrictors at the output of the rate sensor to null system outputs on controllers 2 and 15. Both resistors were placed on the left side, shifting rate-sensor output by 80 to 100 degrees per second in the counterclockwise direction. This shift was necessary to make the rate-sensor amplifier operate in its linear range. Controller 8 received an additional rate-sensor coupling element to reduce system noise. The stackup of tolerances in this case required that 35 coupling elements be used to tightly fill the sensor cavity (all other systems used 34 elements).

The performances of the calibrated systems are summarized in Table 10. All controllers met requirements of gain, response, and noise with fluid temperature at 120°F. Also, one controller from each lot was tested (gain, noise, response) with fluid temperatures from 80° to 180°F. System rate gain as a function of fluid temperature is shown in Figure 19. Controller 7 was calibrated with a higher rate gain, and this difference is even more noticeable at the higher fluid temperatures. Performance was similar for all controllers. PID gain as a function of fluid temperature is shown in Figure 20. Controllers 1 and 16 have similar patterns of PID gain as a function of fluid temperature, while controllers 7 and 14 have slightly different patterns; however, they all remain within a relatively narrow band.

TABLE 10. SUMMARY OF SYSTEM TEST RESULTS

Parameter	Requirement	Controller Serial Number																		
		01	02	03	04	05	06	07	08	09	10	11	12	13	14	15	16	17	18	19
High-pass Rate Gain at 3.0 Hz	0.2 psid/deg/sec Max. 0.127 psid/deg/sec Min.	0.151	0.155	0.160	0.175	0.148	0.170	0.178	0.150	0.145	0.143	0.168	0.168	0.154	0.158	0.149	0.154	0.153	0.157	0.151
Through-rate Gain	0.034 psid/deg/sec Max. 0.021 psid/deg/sec Min.	0.030	0.028	0.030	0.025	0.025	0.032	0.032	0.029	0.027	0.027	0.028	0.032	0.025	0.028	0.030	0.030	0.030	0.032	0.030
PID Gain	42 psid/in. Max. 25 psid/in. Min.	29.0	33.0	34.5	33.0	29.0	33.5	30.5	32.0	33.0	33.2	32.0	38.0	34.0	35.0	29.5	35.3	40.0	32.0	35.0
Noise at 120°F	±0.2 psid Max.	±0.10	±0.05	±0.20	±0.07	±0.20	±0.12	±0.02	±0.10	±0.10	±0.10	±0.08	±0.10	±0.15	±0.05	±0.06	±0.05	±0.13	±0.02	±0.05
Noise at 180°F	No Requirement, psid.	±0.08	NDR	NDR	NDR	NDR	NDR	±0.20	NDR	NDR	NDR	NDR	NDR	NDR	±0.30	NDR	±0.10	NDR	NDR	NDR
Offset	±0.4 psid Max.	0.15	0.05	0.20	0.22	0.25	0.02	0.08	0.12	0.10	0.00	0.10	0.00	0.05	0.10	0.07	0.27	0.34	0.15	0.10
		Lot A					Lot B					Lot C					Lot D			

NDR = No Data Required.

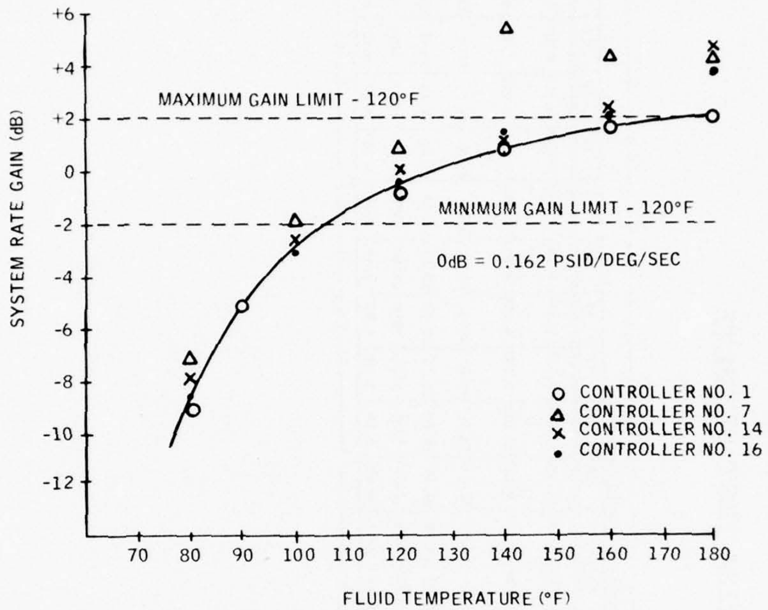

Figure 19. Rate Gain as a Function of Fluid Temperature.

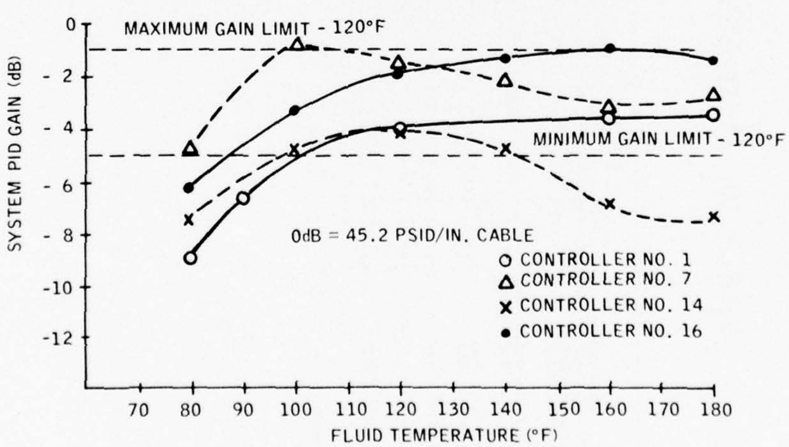

Figure 20. System PID Gain as a Function of Fluid Temperature.

SECTION V
DATA ANALYSIS

A report on the complete statistical analysis of all components electroformed in this phase is presented in Appendix B. This report is reproduced in its entirety, including conclusions and recommendations. These recommendations are combined with other system considerations, and the recommendations that resulted are presented in this section.

The initial yields of rate sensors and integrated circuits will be about 90 percent when the Appendix B recommendations are implemented. It is reasonable to assume that yields will improve substantially with production experience to a level of 95 percent or better on these two components. Eliminating the previously discussed mechanical weaknesses in the through-rate resistors should result in a nearly 100-percent yield on these devices. Recommendations for changes in the integrated circuit specification are summarized in Table 11. Rate-sensor amplifier and PID amplifier requirements in this table are essentially the same as those recommended in the statistical analysis (Appendix B). Present output cascade requirements define the performance of each component in this complex circuit. However, the recommended requirement specifies the cumulative effect of performance variations in bias resistors, amplifiers, through-rate resistors, and feedback resistors. This simplification in the requirements minimizes the amount of testing. Complete testing of the rejected units in accordance with the existing specification would be required to determine which component(s) caused the circuit to be out of limits.

The rate sensor's performance when flow-loaded is typical of its operation in a system, whereas its dead-ended performance data is only

TABLE 11. RECOMMENDED INTEGRATED CIRCUIT REQUIREMENTS

Circuit	Parameter	Present Requirement	Recommended Requirement
Rate Sensor	Null (ΔP_5)	±0.5 psid	±0.5 psid
	Range	±1.0 psid	±1.0 psid
	Reversal (input required)	±0.5 psid	±0.5 psid
	Gain	3.9 ±0.5	4.3 ±0.6
	Noise	0.03 psid max.	0.03 psid max.
	Linearity	±0.15 psid	±0.15 psid
	Pressure Level 7-1 (at input side of C1)	5.0 ±1.0 psid	5.8 ±1.0 psid
PID Amplifier	Null (ΔP_5)	±0.5 psid	±0.5 psid
	Range	±1.0 psid	±1.0 psid
	Gain	3.6 ±0.5	3.3 ±0.5
	Linearity	±0.15 psid	±0.15 psid
Output Cascade	Null (ΔP_6)	0.06 psid max.	None
	Null (ΔP_4) (no feedback)	0.10 psid max.	None
	Null (ΔP_4) (feedback)	None	±0.2 psid max.
	Range (ΔP_3 input)	±2.5 psid	None
	Range (ΔP_4 input)	±1.0 psid	±1.0 psid
	Gain ($\Delta P_{10}/\Delta P_6$)	54 ± 11	None
	Gain ($\Delta P_{10}/\Delta P_4$) (no feedback)	11 ± 1.8	None
	Gain ($\Delta P_{10}/\Delta P_4$) (feedback)	None	7 ± 1
	Gain ($\Delta P_{10}/\Delta P_3$) (no feedback)	19 ± 4	None
	Gain ($\Delta P_{10}/\Delta P_3$) (feedback)	9.2 ±1.4	None
	Noise	0.4 psid max.	0.4 psid max.
	Linearity (ΔP_3)	±0.3 psid max.	None
	Linearity (ΔP_4) (no feedback)	±0.15 psid max.	None
	Linearity (ΔP_4) (feedback)	None	±0.15 psid max.
	Pressure level P 7-2 (at output side of C1)	5.0 ± 1.0 psid	5.8 ±1.0

supplemental information indicating potential causes for unusual flow-loaded performance. Once the sensor is set up in the test fixture, the dead-ended data can be obtained with a minimum of extra effort. It is recommended that the dead-ended gain requirement be retained for the present time, but its tolerance should be increased from ± 0.001 to ± 0.002 psid/deg/sec. The narrow confidence interval for the dead-ended gain should tend to encourage the detection of minor changes in the electroforming process before they become gross enough to reduce yield. Any sensor that fails to pass dead-ended gain requirements will probably also be considerably outside of the flow-loaded limits.

Recommended rate sensor specification changes are:

Dead-ended gain: Change from 0.0090 ± 0.0010 psid/deg/sec
to 0.0090 ± 0.0020 psid/deg/sec

Flow-loaded gain: Change from 0.0050 ± 0.0010 psid/deg/sec
to 0.0050 ± 0.0015 psid/deg/sec

Flow-loaded null offset: Add ± 75 deg/sec

SECTION VI
PRODUCTION COST ESTIMATE

GENERAL

This section presents an estimate of the costs to qualify and manufacture quantities of the OH-58 HYSAS sensor/controller package developed in this program.

The costs presented below are in 1976 dollars. In addition, advancement in the technology and expected improvements in production techniques are expected to reduce manufacturing costs in the future.

RECURRING COSTS

	Quantities 50	Quantities 1000
Units per Month	5	20
Cost per unit (1976 dollars)	4900	2900

NONRECURRING COSTS

The recurring costs assume that the units are fabricated using the pilot production line established in this program: the ECW line plus test equipment (see USAAMRDL-TR-75-49).[1] With this assumption, the following represent the projected additional nonrecurring costs for either quantity.

Non-ECW Tooling and Production Start-Up	$28,600
Qualification	$60,200
TOTAL	$88,800

SECTION VII
CONCLUSIONS AND RECOMMENDATIONS

CONCLUSIONS

- Electroformed components can be fabricated in large quantities with high degrees of repeatability and with initial yields of 90 percent for complex circuits and nearly 100 percent for simple devices, such as feedback-resistor networks. With normal process refinements and operator skill improvements, yields should increase to more than 95 percent for complex devices.
- The ECW process in conjunction with existing conventional processes is suitable for quantity production of fluidic systems.

RECOMMENDATIONS

- Modify the rate sensor and integrated circuit specifications in accordance with the recommendations in Section V, Data Analysis.
- Conduct tests on all components produced, but simplify the integrated circuit tests as recommended in Section V.
- Perform detailed integrated circuit tests (as defined in the present specification) on a small sample of production hardware and on all units that fail to meet the revised specification. Conduct failure analyses on all rejects to exactly determine causes of malfunctions.
- Electroform all resistors into the integrated circuits. Consistency of electroformed resistors is better than that of punched or machined resistors.

- Add gain and null adjustments to simplify calibration, but with limited authority. Sufficient range should be provided to calibrate about 95 percent of the systems without the addition of replaceable resistors.

- Use a plating anode area equal to that of the surface being plated, especially when plating pickoffs. Use a constant-current power supply and monitor voltage with a strip-chart recorder during the entire process.

APPENDIX A

LIST OF DRAWINGS AND SPECIFICATIONS

TABLE A-1. CONTRACTOR DRAWINGS

Drawing Size	Document Number	Sheet Number	Rev. Ltr. Issue Symbol	Nomenclature
E	YG1158A	2	B	Hydrofluidic Yaw Damper System
D	C13789AA01		A	Schematic Diagram
C	10040030		D	Coupling, Element
C	10040250		C	Spool
C	10040251		D	Sleeve
B	10040762		B	Pin
B	10040763		B	Sleeve
C	10047089		A	Orifice
B	10047171		A	Bellows
B	10047181		C	Bellows
B	10047182		A	Valve
C	10047183		A	Cable
C	10047435		F	Lock, Lever
C	10047438		B	Plug
C	10047440		D	Pin, Spool Link
B	10047441		E	Pin, Spool End
C	10047443		C	Arm, Spool Adv
C	10047444		B	Bracket, Support
C	10049016		A	Bellows
C	10049197		A	Bearing
C	10049198		C	Clevis
C	10049200		C	Bar, Mounting
C	10049202		B	Spring
C	10049570		B	Guide
E	10050019		C	Insert
E	10050020		A	Manifold Assy
E	10050021		F	Plate, Manifold
E	10050022	3	E	Manifold, Amplifier
C	10050023		F	Base, Plate, Resistor
C	10050024		E	Block, Outlet
E	10050025	2	M	Housing, Controller
C	10050026		B	Bellow Assy
B	10050027		D	Cover, Capacitor
B	10050028		D	Cover, Capacitor
B	10050029		D	Cover, Capacitor
B	10050030		A	Bellow Assy
B	10050031		C	Cap, Filter
C	10050032		D	Bracket, Null Adjust
C	10050036		D	Cover, VRS Bottom
B	10050037		D	Cover, Blank
C	10050038		A	Hanger, Mounting
C	10050039		A	Bracket, Cable
C	10050040			Plate, Pivot
C	10052137		A	Cover, VRS Top
E	10056117			Insert
C	10058162			Pick Off Assy
B	10058163			Shim
C	10058164			Screw, Shoulder
E	10058165			Cavity, Resistor
D	10058166			Cavity, Resistor
C	10058167			Plate, Identification

TABLE A-2. GOVERNMENT SPECIFICATIONS AND STANDARDS

Drawing Size	Document Number	Sheet Number	Rev. Ltr. Issue Symbol	Nomenclature
	Mil-D-1000			Drawings
	Mil-S-5059			Steel
	Mil-C-5541			Chem Conversion
	Mil-A-8625			Anodic Coatings
	Mil-P-19834			Plate Identification
	Mil-S-22473			Sealing
	MIL-N-45938/7			Nut, Self Locking Clinch
	QQ-A-200/3			Aluminum
	QQ-A-225/6			Aluminum
	QQ-A-250/4			Aluminum
	QQ-A-250/8			Aluminum
	QQ-P-35			Passivation
	QQ-S-571			Solder
	QQ-S-763			Steel
	QQ-S-764			Steel
	QQ-S-766			Steel
	Mil-Std-100			Drawing Practices
	AN 3			Bolt
	AN 814			Plug and Bleeder
	MS16555			Pin, Straight
	MS21209			Insert, Helical
	MS24693			Screw
	MS28775			Packing Preform
	MS33537			Insert
	MS35812			Clevis
	MS51527			Elbow

TABLE A-3. INDUSTRIAL SPECIFICATIONS

Drawing Size	Document Number	Sheet Number	Rev. Ltr. Issue Symbol	Nomenclature
	AMS4017			Aluminum
	AMS4037			Aluminum
	AMS4507			Brass
	AMS4610			Brass
	AMS4805			Bronze
	AMS5610			Steel
	AMS5640			Steel
	NAS43			Spacer, Screw and Bolt
	NAS662			Screw
	NAS1291			Nut, Self Locking
	NAS1352			Screw, Cap
	MC7777-01			Adhesive
	PC13405-01			Adhesives
	PC13502-01			Fluidic Hardware Fabrication by Electroforming
	DS24947-01			Yaw Axis Hydrofluidic Stability Augmentation Sys.
	DS24949-01			Hydraulic Vortex Rate Sensor Pickoff
	DS24950-01			Hydraulic Integrated Amplifier Manifold Circuit
	DS25515-01			Pedal Input Device

APPENDIX B
ENGINEERING TEST REPORT

BACKGROUND

Twenty systems were required to build four groups during Phase III of this program. These systems were tested to determine the producibility of the system and the attainability of the specifications.

CONCLUSIONS

The 95-percent confidence interval of the dead-ended rate sensor's gain was 0.00905 ± 0.00159 psid/deg/sec.

The rate sensor's dead-ended gain appears to be more sensitive to variation than the flow-loaded gain; therefore, measurement of this parameter should be continued.

The 95-percent confidence interval of the flow-loaded rate sensor's gain was 0.00485 ± 0.00209 psid/deg/sec. In production, this may be a yield-limiting parameter.

The 95-percent confidence interval of the null offset was 20.4 ±55.1 deg/sec.

The 95-percent confidence interval of the output cascade, $\Delta P_{10}/\Delta P_6$, was 52.5 ±12.7 psid/psid. This indicates that the limits of 54 ±11 psid/psid are probably too tight.

The noise in the output cascade alone is well below specification levels, and no problem is expected from this source.

The 95-percent confidence interval for the output cascade $\Delta P_{10}/\Delta P_3$ is 19.6 ±2.8 psid/psid. This should give a yield greater than 95 percent with the present specification.

The 95-percent confidence interval for the output cascade $\Delta P_{10}/\Delta P_3$ with feedback is 9.96 ±0.76 psid/psid, which is well within the specification limits of 9.2 ±1.4 psid/psid.

The 95-percent confidence interval for the output cascade $\Delta P_{10}/\Delta P_4$ is 13.7 ±2.8 psid/psid. This would cause a high rejection rate based on the present specification.

The 95-percent confidence interval for the null offset of ΔP_4 input is -0.147 ±0.188 psid.

The 95-percent confidence interval for rate amplifier gain is 4.32 ±0.34 psid/psid. This is out of the specification 3.4 ±0.5 psid/psid.

The 95-percent confidence interval for the rate amplifier null offset is 0.29 ±0.26 psid.

The 95-percent confidence interval for the PID amplifier gain is 3.30 ±0.45 psid/psid.

The 95-percent confidence interval for the PID amplifier null offset is 0.01 ±0.40 psid.

As will be discussed in some detail, this phase of the producibility study indicates that an overall yield of 80 to 85 percent may be expected.

RECOMMENDATIONS

Modify the specification for the dead-ended gain of the rate sensor from 0.0094 ±0.0010 psid/deg /sec to 0.0090 ±0.0013 psid/deg/sec.

Keep the specification for the flow-loaded gain of the rate sensor at 0.0050 ±0.0015 psid/deg/sec.

Measure both the dead-ended gain and the flow-loaded gain.

Set the specification for the flow-loaded null offset at ±75 deg/sec.

Modify the specification for the output cascade $\Delta P_{10}/\Delta P_6$ from 54 ±11 to 53 ±13 psid/psid.

Retain the specification for noise in the output cascade at its present level of 0.4 psid maximum.

Retain the specification for the output cascade $\Delta P_{10}/\Delta P_3$ no feedback at 19 ±4 psid/psid.

Modify the specification for the $\Delta P_{10}/\Delta P_3$ output cascade's gain with feedback from 9.2 ±1.4 to 10.0 ±1.4 psid/psid.

Modify the specification for the $\Delta P_{10}/\Delta P_4$ output cascade's gain no feedback from 11.0 ±1.8 to 13.7 ± 3.0 psid/psid.

Change the limit for ΔP_4's null input no feedback from ±0.10 psid maximum to ±0.4 psid maximum.

Change the specification for the rate amplifier's gain from 3.9 ±0.5 to 4.3 ±0.5 psid/psid.

Retain the specification for rate amplifier null offset at ±0.5 psid.

Retain the specification for PID amplifier gain at 3.6 ±0.5 psid/psid.

Retain the specification for PID amplifier null offset at ±0.5 psid.

RESULTS AND DISCUSSION

Rate sensor performance was based upon the dead-ended gain, the flow-loaded gain, and the flow-loaded null offset.

Rate Sensor Dead-Ended Gain

The data for the dead-ended gain is shown in Table B-1. The numbers above the horizontal line are the dead-ended gain individual measurements of the 20 sensors. In all similar tables in this appendix, the four lots are labeled A, B, C, and D, and the individual sensors are labeled 1, 2, 3, 4, and 5. The same order is maintained in all tables so that, where more than one measurement is made on a given device, its lot and number are the same.

In Table B-1 and throughout this appendix the symbols used have the following significance.

$\sum x_i$ represents the sum of individual measurements. At the extreme right are totals referring to all 20 measurements. Under the individual measurements, the sums are the sum of the column of individual (5) measurements.

$\bar{x}$ is the mean of the individual measurements and is obtained from the expression $\sum x_i / N$, where N is the number of individual measurements in the sum.

TABLE B-1. RATE SENSOR DEAD-ENDED GAIN (10^3 X PSID/DEG/SEC)

	Lot				Total
	A	B	C	D	
Sensor 1	9.45	9.50	9.00	9.05	
Sensor 2	9.35	9.50	9.20	9.70	
Sensor 3	9.25	9.50	9.40	8.20	
Sensor 4	7.90	9.40	9.10	9.25	
Sensor 5	9.60	9.50	9.60	6.50	
Σx_i	45.55	46.40	46.30	42.70	180.95
$\bar{x}$	9.11	9.28	9.26	8.54	9.05
s^2	0.474	0.192	0.058	1.597	0.584
s	0.688	0.438	0.241	1.26	0.76
95% C.I.	±1.91	±1.21	±0.67	±3.50	±1.59
Interval	7.2 to 11.0	8.1 to 10.5	8.6 to 10.0	5.0 to 12.0	7.46 to 10.64

s^2 is the variance of the individual measurements. It is calculated from the equation:

$$s^2 = \frac{\Sigma x_i^2 - (\Sigma x_i)^2/N}{N - 1}$$

in which x_i is an individual value and N = the number of measurements.

The variance is indicative of the shape of the distribution curve for normal (or Gaussian) distribution. Although the number of measurements in this study was too small to determine whether the data follows a normal distribution, normal distribution is assumed throughout this report. The symbol s^2 is used for variance rather than σ^2 since this is a best estimate of the parameter, calculated from the data, rather than the universal constant, which would require an infinite number of samples.

s is the standard deviation calculated for the system (square root of the above variance).

95% C.I. is the 95-percent confidence interval of the data. This means that, if a sample were drawn at random from the universe represented by this data, there is a 95-percent probability that it would be within these limits. It is calculated from the equation:

$$95\%\ \text{C.I.} = s \cdot t_{0.05}$$

in which s is the standard deviation and $t_{0.05}$ is the Student t value taken from tabular data. This value, t , allows a correction for sample size. If an infinitely large sample were used, $t_{0.05}$ would be 1.96. For a sample size of four, the value of $t_{0.05}$ is 3.18. For smaller samples, t increases rapidly such that, for a sample size of 2, $t_{0.05} = 12.71$.

The interval shown is the actual limits of the 95-percent confidence interval and is shown for convenience only.

To determine whether the variance within lots was significantly less than the variance between lots, a one-way classification was used to calculate the variances.[3]

These calculations were made as follows:

$$\text{Correction factor} = (\Sigma x_i)^2/N = 1637.1451$$

$$\text{Crude lot SS} = [(45.55)^2 + (46.40)^2 + (46.30)^2 + (42.70)^2]/5 = 1638.9485$$

---

[3] C.A. Bennett and N.L. Franklin, Statistical Analysis in Chemistry and the Chemical Industry, New York, John Wiley and Sons Inc., 1954, pp 321-329.

$$\text{Total SS} = \Sigma x_i^2 - (\Sigma x_i)^2/N = 1648.2325 - 1637.1451 = 11.0874$$

$$\text{Lot SS} = \Sigma T_i^2/N - (\Sigma x_i)^2/N = 1638.9485 - 1637.1451 = 1.8034$$

$$\text{Within Lot SS} = 11.0874 - 1.8034 = 9.2840$$

In these calculations:

Σx_i = the sum of all 20 data points

N = the number of data points

SS = the sum of squares

The crude lot sum of squares is equal to:

$$\Sigma_i T_i^2/N$$

in which T_i is the sum of the values for the five samples in each lot.

Lot SS = Crude Lot SS - correction factor

$$\text{Total SS} = \Sigma x_i^2 - (\Sigma x_i)^2/N$$

in which x_i is an individual data point.

Within Lot SS = Total SS - Lot SS

The analysis of variance is summarized in Table B-2.

TABLE B-2. RATE SENSOR DEAD-ENDED GAIN ANALYSIS OF VARIANCE

Source	SS	df	MS	Ratio	$F_{\alpha=0.05}$
Lot	1.8034	3	0.6011	1.04	3.24
Within Lot	9.2840	16	0.5803		
Total	11.0874	19	0.5835		

The analysis of variance is a method of separating the variance from various sources and testing for statistical significance.

The headings in this analysis of variance table, and others like it, are used as follows:

SS is the sum of squares calculated as shown above.

df is the degrees of freedom. The total degrees of freedom (19) is N - 1 where N = the number of data points. The lot-to-lot degrees of freedom (3) is the number of lots minus 1. The degrees of freedom within lots (16) is the difference between total degress of freedom and lot-to-lot degrees of freedom.

MS is the mean square and is obtained by dividing the sum of squares by the degrees of freedom. The ratio of the mean squares (0.6011/0.5803 = 1.04) is used to determine statistical significance. This ratio is compared to the tabular F value, which is the ratio required at a given probability level. It is dependent upon the degrees of freedom of the two mean squares. Thus, the required ratio for significance of two mean squares with 3 and 16 degrees of freedom, respectively, is 3.24 at a 95-percent probability level. When the ratio of mean squares is larger than the tabular F value, there is a statistically significant indication that the performance is changing from lot to lot at the confidence interval selected (in this case 95%).

From Table B-2 it is seen that there is no significant difference between lot-to-lot variation and within-lot variation at the 95-percent probability level. This means that, for the system, all data points can be combined to give a standard deviation for part-to-part deviation.

The study was not designed to separate testing error from process variability; therefore, the standard deviation shown includes both testing error and process variability. Data on replicate testing would be required to separate these two sources of variability.

Throughout this report, 95-percent probabilities were selected to determine significance. The reason this level was selected is because there are two types of errors that are related. An error of the first kind (which we have taken at 95 percent) involves the hypothesis that there is a difference when no actual difference exists. An error of the second kind involves the hypothesis that there is no difference when a real difference exists. When the error of the first kind has a probability of 95 percent, the error of the second kind has a probability of 90 percent. This represents a reasonable balance and is the reason the 95-percent probability level is normally selected.

From Table B-1 it is seen that, in drawing a sample from the universe represented by this data, there is a 95-percent probability that the dead-ended gain will lie between 0.00746 and 0.01064. This represents a range of ±17.6 percent of the mean value.

Flow-Loaded Gain

The data for flow-loaded gain is shown in Table B-3. The format of this table is the same as that used in Table B-1.

TABLE B-3. RATE SENSOR FLOW-LOADED GAIN
(10^3 X PSID/DEG/SEC)

	Lot				Total
	A	B	C	D	
Sensor 1	4.95	5.10	3.90	5.10	
Sensor 2	5.40	6.25	5.15	6.20	
Sensor 3	4.35	5.50	4.00	4.55	
Sensor 4	3.50	5.00	3.75	5.15	
Sensor 5	5.40	5.30	4.70	3.70	
$\sum x_i$	23.60	27.15	21.50	24.70	96.95
$\bar{x}$	4.72	5.43	4.30	4.94	4.85
s^2	0.651	0.247	0.359	0.837	0.615
s	0.81	0.50	0.60	0.91	0.78
95% C.I.	±2.24	±1.38	±1.66	±2.53	±2.09
Interval	2.5 to 6.9	4.0 to 6.8	2.6 to 6.0	2.4 to 7.4	2.76 to 6.94

The variances between lots and within lots were calculated as follows:

$$\text{Correction Factor} = (\sum x_i)^2/N = 469.9651$$

$$\text{Crude Lot SS} = \sum_i T_i^2/N = [(23.60)^2 + (27.15)^2 + (21.5)^2 + (24.7)^2]/5$$
$$= 473.2845$$

$$\text{Total SS: } \sum x_i^2 - (\sum x_i)^2/N = 481.6575 - 469.9651 = 11.6924$$

$$\text{Lot SS} = \sum T_i^2/N - (\sum x_i)^2/N = 473.2845 - 469.9651 = 3.3194$$

$$\text{Within Lot SS: } 11.6924 - 3.3194 = 8.3730$$

The analysis of variance is summarized in Table B-4.

TABLE B-4. RATE SENSOR FLOW-LOADED GAIN ANALYSIS OF VARIANCE

Source	SS	df	MS	Ratio	$F_{\alpha=0.05}$
Lot	3.3194	3	1.1065	2.11	3.24
Within Lot	8.3730	16	0.5233	---	
Total	11.6924	19	0.6154		

When comparing the ratio of the mean squares with the F value for 3 and 16 degrees of freedom, it is seen that, at the 95-percent confidence interval, the variance between lots is not significantly different from that within lots. As previously stated, the data does not permit the separation of testing error from sample-to-sample variation.

From Table B-3 it is seen that, if a sample is drawn from the universe represented by this data, there is a 95-percent probability that the flow-loaded gain would be between 0.00276 and 0.00694. This represents a range of 43 percent of the mean value. There is a 90-percent probability that the flow-loaded gain would lie within a range of ±30 percent. This indicates that with the present specification the expected yield, due to this factor, would be about 90 percent.

Two of the rate sensors were considered out of line, both on the basis of the dead-ended gain and on the basis of the flow-loaded gain. These two (the fourth sample in Lot A and the fifth sample in Lot D) were not used in any completed device. However, they were included in the statistical analysis of the data, because there was no indication of abnormalities that would have justified omitting them. With these two devices omitted from the data, the mean and 95-percent confidence intervals would have been 0.00925 ±0.00038 (8.8 percent) for the dead-ended gain and 0.00499 ±0.00070 (29.4 percent) for the flow-loaded gain.

In any case, the flow-loaded gain shows significantly larger variability than the dead-ended gain.

Flow-Loaded Null Offset

The data for the flow-loaded null offset of the rate sensor is summarized in Table B-5. Counterclockwise adjustments are indicated by minus signs in this table.

TABLE B-5. RATE SENSOR FLOW-LOADED NULL OFFSET (DEGREES PER SECOND)

	Lot				Total
	A	B	C	D	
Sensor 1	-32.0	-15	+28	-11.0	
Sensor 2	+10.0	+6	+13	-4.5	
Sensor 3	+7.5	+49	-24	+69.5	
Sensor 4	+17.0	+43	+42	+66.0	
Sensor 5	+8.0	+21	+25	+42.0	
Σx_i	+10.50	104.00	84.00	162.00	408.500
$\bar{x}$	+2.10	+20.80	16.80	32.40	20.420
s^2	377.80	697.20	626.70	1460.68	692.165
s	19.44	26.40	25.03	38.22	26.310
95% C.I.	54.00	73.30	69.08	106.10	55.070
Interval	-51.9 to +56.1	-52.4 to +94.1	-2.5 to +55.3	-73.7 to +138.5	-34.6 to +75.5

The variances between lots and within lots were calculated as follows:

Correction Factor = $(\Sigma x_i)^2/N$ = 8343.6125

Crude Lot SS: $\Sigma_i T_i^2/N = [(10.5)^2 + (104)^2 + (84)^2 + (162)^2]/5$
$= 8845.25$

Total SS: $\Sigma x_i^2 - (\Sigma x_i)^2/N = 21494.75 - 8343.61 = 13151.14$

Lot SS: $\Sigma_i T_i^2/N - (\Sigma x_i)^2/N = 8845.25 - 8343.61 = 501.64$

Within Lot SS: Total SS - Lot SS = 13151.14 - 501.64 = 12649.50

The analysis of variance is summarized in Table B-6.

TABLE B-6. RATE SENSOR FLOW-LOADED NULL OFFSET ANALYSIS OF VARIANCE

Source	SS	df	MS	Ratio	$F_{\alpha=0.05}$
Lot	501.64	3	167.21	0.21	3.24
Within Lots	12649.50	16	790.59	---	
Total	13151.14	19	692.16	---	

There is no significant difference between lot-to-lot variance and within-lot variance at the 95-percent confidence interval.

There is a wide variability in the null offset. The 95-percent confidence interval is 34.6 deg/sec counterclockwise to 75.5 deg/sec clockwise, which represents 270 percent of the mean value.

To summarize the data for the hydrofluidic vortex rate sensor: The data for the dead-ended gain may not be normally distributed, although the sample size is too small to evaluate this factor. It may be that a single-tailed test should be applied, since the possible value may reach a maximum value at about 9.7, which appears to skew the curve to the left. The specification of 0.0094 ±0.0010 psid/deg/sec may be too rigid and could result in a 60-percent yield. Because all of the parts yielded systems that could be calibrated, the yield could be increased to 90 percent by changing the specification to 0.0090 ±0.0013 psid/deg/sec. A further change to 0.0090 ±0.0015 psid/deg/sec would result in approximately a 95-percent yield.

The data on the flow-loaded gain is significantly more variable than the data on the dead-ended gain. Again, the specification is tight, and a yield of about 90 percent would be expected from these specifications. It is interesting to note that, using the current specifications, none of the 20 rate sensors would have been rejected on this parameter. A

change in specification to 0.0048 ±0.0021 psid/deg/sec would be required to obtain a 95-percent probability of obtaining an acceptable part. However, this may be too wide a range to yield systems capable of being calibrated. One would be inclined to keep the specification as written for this parameter, unless further evaluation is made with this factor at levels of 0.0027 psid/deg/sec.

The flow-loaded null offset varied widely from a mean value of 20.4 deg/sec clockwise. Because this does not appear to be a problem, the limits should probably be set wide enough so that few units will be rejected on this basis. The 95-percent confidence limits are 20.4 ±55.1 deg/sec. Whether future builds will have a mean in the clockwise direction is unknown, but these confidence limits are probably minimal. One could probably get by with limits of ±75 deg/sec.

Output Cascade Gain

The data for the output cascade gain $\Delta P_{10}/\Delta P_6$ are shown in Table B-7.

TABLE B-7. OUTPUT CASCADE GAIN $\Delta P_{10}/\Delta P_6$ (PSID/PSID)

	Lot				Total
	A	B	C	D	
Sensor 1	55.90	58.06	53.19	54.59	
Sensor 2	54.54	59.17	52.63	52.63	
Sensor 3	47.14	31.31	54.94	51.68	
Sensor 4	47.50	53.33	53.61	54.05	
Sensor 5	57.05	50.00	56.70	---	
Σx_i	262.13	251.87	271.07	212.85	997.92
$\bar{x}$	52.43	50.37	54.21	53.24	52.53
s^2	22.5316	127.1895	2.6574	1.7614	36.35
s	4.75	11.28	1.63	1.33	6.02
95% C.I.	±13.2	±31.3	±4.5	±4.2	±12.7
Interval	39.2 to 65.6	19.1 to 81.7	49.7 to 58.7	49.1 to 57.3	39.8 to 65.2

The variances between lots and within lots were calculated as follows. (It should be noted that a modified calculation was made for determining the crude lot-to-lot sum of squares. This was required due to the missing value in Lot D.)

$$\text{Correction Factor} = (\Sigma x_i)^2/N = 52412.85928$$

$$\text{Crude Lot SS: } \Sigma_i(T_i^2/N_i) = (262.13)^2/5 + (251.87)^2/5 + (271.07)^2/5 + (212.85)^2/4 = 52452.1964$$

$$\text{Total SS: } \Sigma x_i^2 - (\Sigma x_i)^2/N = 53066.7318 - 5412.8593 = 653.8725$$

$$\text{Lot SS: } \Sigma_i(T_i^2/N_i) - (\Sigma x_i)^2/N = 52452.1964 - 52412.8593 = 39.3371$$

$$\text{Within Lot SS: Total SS} - \text{Lot SS} = 653.8527 - 39.3371 = 614.5354$$

The analysis of variance is summarized in Table B-8.

TABLE B-8. OUTPUT CASCADE GAIN $\Delta P_{10}/\Delta P_6$ ANALYSIS OF VARIANCE

Source	SS	df	MS	Ratio	$F_{\alpha=0.05}$
Lot	39.3371	3	13.1124	0.32	3.29
Within Lots	614.5354	15	40.9690		
Total	653.8725	18	36.3262		

The fact that the ratio of mean squares is less than 1 is due to the extremely low value in Lot B. Thus, obviously there is no significant difference in variance between lots and within lots.

In the analysis of variance, several basic assumptions are made:

- The various effects are additive.
- The experimental errors must be independent of the main effects and interactions and of each other.
- The experimental errors must have a common variance.
- The experimental errors must be randomly and normally distributed.

The F ratio is expected to be greater than 1. When this is not true, as in the present case, one is led to suspect that the model chosen is incorrect. This may be caused by failure of the assumption that the experimental error, which in our present study is represented by within-lot variation, is randomly and normally distributed. The assumption might fail because the tests were not made in random order. Any effects of chronological sequence would increase the within-lot estimate of variance, while leaving the between-lot estimate unaffected. This would reduce the variance ratio and might account for the low F ratios calculated in this case and in several other cases in this study.

From Table B-7 it is seen that the output cascade gain is 52.5 ±12.7 at the 95-percent confidence interval. Using the limits set in the specification, this would give a yield of slightly greater than 90 percent Because all of the systems were capable of calibration, this specification is probably too tight. It should probably be changed to 53 ±13, which would give a yield slightly greater than 95 percent.

Output Cascade Noise Data

The output cascade noise data is shown in Table B-9.

TABLE B-9. OUTPUT CASCADE NOISE (PSID X 10^3)

	Lot				Total
	A	B	C	D	
Sensor 1	15.0	14	3	12	
Sensor 2	50.0	14	18	---	
Sensor 3	34.5	33	14	---	
Sensor 4	3.0	41	16	---	
Sensor 5	3.0	30	---	---	
$\sum x_i$	105.5	132.0	51.0	12	300.5
$\bar{x}$	21.1	26.4	12.8	12	20.0
s^2	426.8	144.3	44.9	---	207.4
s	20.6	12.0	6.7	---	14.4
95% C.I.	57.2	33.3	21.3	---	30.9
Interval*	0 to 0.0783	0 to 0.0597	0 to 0.0341	---	0 to 0.0509

* Data in this interval is not multipled by 10^3.

The variances between lots and within lots were calculated as follows:

$$\text{Crude Lot SS} = \Sigma_i (T_i^2/N_i) = (105.5)^2/5 + (132)^2/5 + (51)^2/4 = 6361.1$$

$$\text{Correction Factor} = (\Sigma x_i)^2/N = 6020.0167$$

$$\text{Total SS: } \Sigma x_i^2 - (\Sigma x_i)^2/N = 8924.25 - 6020.0167 = 2904.2333$$

$$\text{Lot SS: } \Sigma_i (T_i^2/N_i) - (\Sigma x_i)^2/N = 6361.1 - 6020.0167 = 341.0833$$

$$\text{Within Lot SS: Total SS} - \text{Lot SS} = 2904.2333 - 341.0833 = 2563.15$$

The analysis of variance is summarized in Table B-10.

TABLE B-10. OUTPUT CASCADE NOISE ANALYSIS OF VARIANCE

Source	SS	df	MS	Ratio	$F_{\alpha=0.05}$
Lot	341.0833	2	170.5417	0.80	3.89
Within Lot	2563.1500	12	213.5958	---	
Total	2904.2333	14	207.4400		

Examination of Table B-10 shows there is no significant difference at the 95-percent probability level between the variances between lots and within lots.

The 95-percent confidence interval for noise is 0.0200 ±0.0309, as shown in Table B-9. Therefore, as the specification requirement is that the noise level be less than 0.4, no problems are expected from this factor. This specification could be tightened by almost a factor of 10 if noise near the specification limit is a problem, but if no problems are noted, it would be advisable to leave the specification for noise as written, and expect no problems in meeting it.

Gain - Output Cascade $\Delta P_{10}/\Delta P_3$ Without Feedback

The data for the gain of the output cascade $\Delta P_{10}/\Delta P_3$ is summarized in Table B-11.

TABLE B-11. GAIN - OUTPUT CASCADE $\Delta P_{10}/\Delta P_3$ WITHOUT FEEDBACK (PSID/PSID)

	Lot				Total
	A	B	C	D	
Sensor 1	19.59	20.50	19.57	20.49	
Sensor 2	21.18	20.80	19.07	20.83	
Sensor 3	17.41	15.99	20.75	20.00	
Sensor 4	17.74	19.52	19.72	20.20	
Sensor 5	20.34	19.31	18.59	---	
$\sum x_i$	96.26	96.12	97.70	81.52	371.60
$\bar{x}$	19.25	19.22	19.54	20.38	19.56
s^2	2.6736	3.6664	0.6552	0.1305	1.7835
s	1.64	1.91	0.81	0.36	1.33
95% C.I.	4.5	5.3	2.2	1.1	2.8
Interval	14.7 to 23.7	13.9 to 24.5	17.3 to 21.7	19.3 to 21.5	16.8 to 22.4

The variances between lots and within lots were calculated as follows:

$$\text{Crude Lot SS} = \sum_i (T_i^2/N_i) = \frac{(96.26)^2}{5} + \frac{(96.12)^2}{5} + \frac{(97.70)^2}{5}$$

$$+ \frac{(81.52)^2}{4} = 7271.4440$$

$$\text{Correction Factor} = (\sum x_i)^2/N = 7267.7137$$

$$\text{Total SS} = \sum x_i^2 - (\sum x_i)^2/N = 7299.8162 - 7267.7137 = 32.1025$$

$$\text{Lot SS} = \sum_i (T_i^2/N_i) - (\sum x_i)^2/N = 7271.4440 - 7267.7137 = 3.7303$$

$$\text{Within Lot SS} = \text{Total SS} - \text{Lot SS} = 32.1025 - 3.7303 = 28.3722$$

The analysis of variance is summarized in Table B-12.

TABLE B-12. GAIN-OUTPUT CASCADE $\Delta P_{10}/\Delta P_3$ ANALYSIS OF VARIANCE

Source	SS	df	MS	Ratio	$F_{\alpha=0.05}$
Lot	3.7303	3	1.2434	0.66	3.29
Within Lot	28.3722	15	1.8915	---	
Total	32.1025	18	1.7835		

There is one exceptionally low value (number 3 in Lot B) that probably accounts for a ratio of mean squares less than 1. Thus, the lot-to-lot variance is not significantly different from the within-lot variance.

A constant ratio is expected between the gain measured for $\Delta P_{10}/\Delta P_6$ and that measured for $\Delta P_{10}/\Delta P_3$. The ratios for the different lots are compared in Table B-13.

TABLE B-13. RATIO BETWEEEN GAINS MEASURED FOR $\Delta P_{10}/\Delta P_6$ AND $\Delta P_{10}/\Delta P_3$

	Gain $\Delta P_{10}/\Delta P_6$	Gain $\Delta P_{10}/\Delta P_3$	Ratio
Lot: A	52.43	19.25	2.72
B	50.37	19.22	2.62
C	54.21	19.54	2.77
D	53.21	20.38	2.61
Mean	52.56	19.60	2.68

As expected, a constant ratio is obtained between these two values. However, there appears to be more variability in the gain $\Delta P_{10}/\Delta P_6$ than in the gain $\Delta P_{10}/\Delta P_3$. The gain in $\Delta P_{10}/\Delta P_6$ is 52.6 ±12.7 (24.2 percent), whereas the gain in $\Delta P_{10}/\Delta P_3$ is 19.60 ±2.8 (14.3 percent). The specification for gain $\Delta P_{10}/\Delta P_3$ (19 ±4) is quite wide, and based on this factor, a yield greater than 95 percent is expected.

Gain - Output Cascade $\Delta P_{10}/\Delta P_3$ with Feedback

The data obtained for the gain of the output cascade with feedback $\Delta P_{10}/\Delta P_3$ are summarized in Table B-14.

TABLE B-14. GAIN - OUTPUT CASCADE $\Delta P_{10}/\Delta P_3$ WITH FEEDBACK (PSID/PSID)

	Lot				Total
	A	B	C	D	
Sensor 1	10.00	10.20	9.71	10.00	
Sensor 2	10.04	10.10	9.90	10.47	
Sensor 3	9.68	8.97	10.36	9.80	
Sensor 4	9.75	9.76	9.66	10.31	
Sensor 5	10.00	10.10	10.53	---	
Σx_i	49.47	49.13	50.16	40.58	189.34
$\bar{x}$	9.89	9.83	10.03	10.14	9.96
s^2	0.0276	0.2568	0.1538	0.0910	0.1277
s	0.166	0.507	0.39	0.30	0.36
95% C.I.	0.46	1.41	1.08	0.95	0.76
Interval	9.43 to 10.35	8.4 to 11.2	8.9 to 11.1	9.2 to 11.1	9.20 to 10.72

The variances between lots and within lots were calculated as follows:

$$\text{Crude Lot SS} = \Sigma_i(T_i^2/N_i) = \frac{(49.47)^2}{5} + \frac{(49.13)^2}{5} + \frac{(50.16)^2}{5} + \frac{(40.58)^2}{4} = 1887.0968$$

$$\text{Correction Factor} = (\Sigma x_i)^2/N = 1886.8229$$

$$\text{Total SS} = \Sigma x_i^2 - (\Sigma x_i)^2/N = 1889.1222 - 1886.8229 = 2.2993$$

$$\text{Lot SS} = \Sigma_i(T_i^2/N_i) - (\Sigma x_i)^2/N = 1887.0968 - 1886.8229 = 0.2739$$

$$\text{Within Lot SS} = \text{Total SS} - \text{Lot SS} = 2.2993 - 0.2739 = 2.0254$$

The analysis of variance is summarized in Table B-15.

TABLE B-15. GAIN - OUTPUT CASCADE $\Delta P_{10}/\Delta P_3$ WITH FEEDBACK ANALYSIS OF VARIANCE

Source	SS	df	MS	Ratio	$F_{\alpha=0.05}$
Lot	0.2739	3	0.0913	0.68	3.29
Within Lot	2.0254	15	0.1350		
Total	2.2993	18	0.1277		

From Table B-15 it is seen that there is no significant difference between the variance between lots and that within lots at the 95-percent probability level.

From Table B-14 it is seen that the 95-percent confidence interval for $\Delta P_{10}/\Delta P_3$ with feedback is 9.96 ±0.76 (7.6 percent). The specifications would allow greater than 95-percent yield based on this data. The mean value of 9.2 is slightly low and could be increased to 10.0 without affecting the yield significantly.

Gain - Output Cascade $\Delta P_{10}/\Delta P_4$

The data for the output cascade gain $\Delta P_{10}/\Delta P_4$ is summarized in Table B-16.

The variances between lots and within lots were calculated as follows:

$$\text{Correction Factor} = (\textstyle\sum x_i)^2/N = 3572.1405$$

$$\text{Total SS} = \textstyle\sum x_i^2 - (\sum x_i)^2/N = 3603.0924 - 3572.1405 = 30.9519$$

$$\text{Crude Lot SS} = \textstyle\sum_i (T_i^2/N_i) = \frac{(66.50)^2}{5} + \frac{(70.69)^2}{5} + \frac{(66.05)^2}{5} + \frac{(57.28)^2}{4}$$

$$= 3576.6353$$

TABLE B-16. GAIN - OUTPUT CASCADE $\Delta P_{10}/\Delta P_4$ (PSID/PSID)

	Lot				Total
	A	B	C	D	
Sensor 1	15.38	14.29	13.16	14.93	
Sensor 2	14.13	14.08	11.63	12.05	
Sensor 3	12.00	13.89	13.80	15.15	
Sensor 4	10.70	13.51	13.17	15.15	
Sensor 5	14.29	14.92	14.29	---	
Σx_i	66.50	70.69	66.05	57.28	260.52
$\bar{x}$	13.30	14.14	13.21	14.32	13.71
s^2	3.6114	0.2735	1.0038	2.3009	1.7195
s	1.90	0.52	1.00	1.52	1.31
95% C.I.	5.3	1.4	2.8	4.8	2.8
Interval	8.0 to 18.6	12.6 to 15.5	10.4 to 16.0	9.5 to 19.2	10.9 to 16.5

$$\text{Lot SS} = \Sigma_i(T_i^2/N_i) - (\Sigma x_i)^2/N = 3576.6353 - 3572.1405 = 4.4948$$

$$\text{Within Lot SS} = \text{Total SS} - \text{Lot SS} = 30.9519 - 4.4948 = 26.4571$$

The analysis of variance is summarized in Table B-17.

TABLE B-17. GAIN - OUTPUT CASCADE $\Delta P_{10}/\Delta P_4$ ANALYSIS OF VARIANCE

Source	SS	df	MS	Ratio	$F_{\alpha=0.05}$
Lot	4.4948	3	1.4983	0.85	3.29
Within Lot	26.4571	15	1.7638	---	
Total	30.9519	18	1.7196		

From Table B-17 it is seen that at the 95-percent probability level there is no significant difference in the variance between lots from that within lots.

From Table B-16 the 95-percent confidence interval of the gain of the output cascade $\Delta P_{10}/\Delta P_4$ is 13.71 ±2.8 (20.4 percent). The specification for this gain is 11.8 ±1.8 (10.0-13.6). Retaining this specification

will result in an extremely low yield. A yield of greater than 95 percent can be obtained by changing this specification to 13.7 ±3.0. As all of the devices were capable of calibration, this is considered a reasonable modification.

Null Offset of ΔP_4 Input

The data for the null offset of ΔP_4 input is summarized in Table B-18.

TABLE B-18. NULL OFFSET OF ΔP_4 INPUT (PSID)

	Lot				Total
	A	B	C	D	
Sensor 1	-0.1450	-0.132	-0.090	+0.058	
Sensor 2	-0.1375	-0.108	-0.200	-0.188	
Sensor 3	-0.1850	-0.030	-0.178	-0.245	
Sensor 4	-0.0250	-0.183	-0.268	-0.290	
Sensor 5	-0.0880	-0.243	-0.115		
Σx_i	-0.5805	-0.696	-0.851	-0.665	-2.7925
$\bar{x}$	-0.1161	-0.1392	-0.1702	-0.1663	-0.147
s^2	0.0038	0.0064	0.0050	0.0241	0.0079
s	0.062	0.080	0.071	0.16	0.089
95% C.I.	0.172	0.222	0.197	0.509	0.188
Interval	+0.056 to - 0.288	+0.083 to -0.361	+0.027 to -0.367	+0.34 to -0.675	+0.041 to -0.335

The variances between lots and within lots were calculated as follows:

$$\text{Correction Factor} = (\Sigma x_i)^2/N = 0.410424$$

$$\text{Total SS} = \Sigma x_i^2 - (\Sigma x_i)^2/N = 0.5527 - 0.4104 = 0.1423$$

$$\text{Crude Lot SS} = \Sigma_i(T_i^2/N_i) = \frac{(0.5805)^2}{5} + \frac{(0.696)^2}{5} + \frac{(0.851)^2}{5} + \frac{(0.665)^2}{4} = 0.419676$$

$$\text{Lot SS} = \Sigma_i(T_i^2/N_i) - (\Sigma x_i)^2/N = 0.419676 - 0.410424 = 0.009252$$

$$\text{Within Lot SS} = \text{Total SS} - \text{Lot SS} = 0.1423 - 0.009252 = 0.133048$$

The analysis of variance is summarized in Table B-19.

TABLE B-19. NULL OFFSET OF ΔP_4 INPUT ANALYSIS OF VARIANCE

Source	SS	df	MS	Ratio	$F_{\alpha=0.05}$
Lots	0.009252	3	0.003084	0.35	3.29
Within Lots	0.133048	15	0.008868		
Total	0.142300	18	0.007900		

The data in Table B-19 shows that the lot-to-lot variation is not significantly greater than the within-lot variation. The extremely small ratio of these two variances is probably due in part to the fact that the largest and smallest values fell in the same lot (Lot D). It may also indicate that the variation is not completely random.

From Table B-18 the 95-percent confidence interval is seen to be -0.147 ±0.188. A null offset requirement of ±0.4 would give a greater than 95-percent yield.

Rate Amplifier Gain

The data for the gain of the rate amplifier is summarized in Table B-20.

TABLE B-20. RATE AMPLIFIER GAIN (PSID/PSID)

	Lot				Total
	A	B	C	D	
Sensor 1	4.50	4.35	4.27	4.09	
Sensor 2	4.44	4.19	4.14	4.24	
Sensor 3	4.67	4.50	4.13	4.03	
Sensor 4	4.38	4.21	4.38	4.38	
Sensor 5	4.33	4.43	4.42	---	
Σx_i	22.32	21.68	21.34	16.74	82.08
$\bar{x}$	4.46	4.34	4.27	4.18	4.32
s^2	0.01733	0.01828	0.01777	0.02470	0.026611
s	0.1316	0.1352	0.1330	0.1572	0.1631
95% C.I.	0.37	0.37	0.37	0.50	0.34
Interval	4.09 to 4.83	3.96 to 4.71	3.90 to 4.64	3.68 to 4.68	3.98 to 4.66

The variances between lots and within lots were calculated as follows:

$$\text{Correction Factor} = (\Sigma x_i)^2/N = 354.5856$$

$$\text{Crude Lot SS} = \Sigma_i(T_i^2/N_i) = \frac{(22.32)^2}{5} + \frac{(21.68)^2}{5} + \frac{(21.34)^2}{5} + \frac{(16.74)^2}{4}$$

$$= 354.77698$$

$$\text{Total SS} = \Sigma_i^2 - (\Sigma x_i)^2/N = 355.0646 - 354.5856 = 0.4790$$

$$\text{Lot SS} = \Sigma_i(T_i^2/N_i) - (\Sigma x_i)^2/N = 354.77698 - 354.5856 = 0.19138$$

$$\text{Within Lot SS} = \text{Total SS} - \text{Lot SS} = 0.4790 - 0.19138 = 0.28762$$

The analysis of variance is summarized in Table B-21.

TABLE B-21. RATE AMPLIFIER GAIN ANALYSIS OF VARIANCE

Source	SS	df	MS	Ratio	$F_{\alpha=0.05}$
Lots	0.19138	3	0.0638	3.32	3.29
Within Lots	0.28762	15	0.0192		
Total	0.47900	18	0.0266		

The data shown in Table B-21 indicates that there is a significant difference between the lot-to-lot variation and the within-lot variation at the 95-percent probability level. This difference in variability could be due to testing errors from lot-to-lot, process variables from lot-to-lot, or a combination of the two.

The 95-percent confidence interval of the rate amplifier gain is seen to be 4.32 ±0.34 (7.9 percent). Although the variability is quite low, the rate gain of 3.4 ±0.5 set in the specification is too low and would have

resulted in a 100-percent rejection of this lot. Changing the specification to 4.3 ±0.5 would result in a yield greater than 95 percent.

Rate Amplifier Null Offset

The data for the rate amplifier null offset is summarized in Table B-22.

TABLE B-22. RATE AMPLIFIER NULL OFFSET (PSID AT OUTPUT)

	Lot				Total
	A	B	C	D	
Sensor 1	0.30	0.40	0.40	0.20	
Sensor 2	0.25	0.20	0.35	0.10	
Sensor 3	0.65	0.35	0.15	0.30	
Sensor 4	0.30	0.25	0.30	0.35	
Sensor 5	0.25	0.30	0.10	---	
$\sum x_i$	1.75	1.50	1.30	0.95	5.50
$\bar{x}$	0.35	0.30	0.26	0.24	0.289
s^2	0.02875	0.00625	0.01675	0.01229	0.01544
s	0.170	0.079	0.129	0.110	0.124
95% C.I.	0.47	0.22	0.36	0.35	0.26
Interval	-0.12 to +0.82	-0.08 to +0.52	-0.10 to +0.62	-0.11 to +0.59	+0.03 to +0.55

The variances betweeen lots and within lots were calculated as follows:

$$\text{Correction Factor} = (\sum x_i)^2/N = 1.5921$$

$$\text{Crude Lot SS} = \sum_i (T_i^2/N_i) = \frac{(1.75)^2}{5} + \frac{(1.50)^2}{5} + \frac{(1.30)^2}{5} + \frac{(0.95)^2}{4}$$

$$= 1.626125$$

$$\text{Total SS} = \sum x_i^2 - (\sum x_i)^2/N = 1.87 - 1.5921 = 0.2779$$

$$\text{Lot SS} = \sum (T_i^2/N_i) - (\sum x_i)^2/N = 1.626125 - 1.5921 = 0.03402$$

$$\text{Within Lot SS} = \text{Total SS} - \text{Lot SS} = 0.2779 - 0.03402 = 0.24388$$

The analysis of variance is summarized in Table B-23.

TABLE B-23. RATE AMPLIFIER NULL OFFSET ANALYSIS OF VARIANCE

Source	SS	df	MS	Ratio	$F_{\alpha=0.05}$
Lot	0.03402	3	0.01134	0.70	3.29
Within Lot	0.24388	15	0.01626		
Total	0.27790	18	0.01540		

Table B-23 shows that at the 95-percent probability level there is no significant difference between the lot-to-lot variability and the within-lot variability. Again, the fact that the ratio of mean squares is less than 1 may mean that the results are not completely random.

The data in Table B-22 indicates that the 95-percent confidence interval of the rate amplifier null offset is 0.289 ±0.26. Therefore, the specification of ±0.5 would give approximately a 95-percent yield.

PID Gain

The data for PID gain is summarized in Table B-24.

TABLE B-24. PID AMPLIFIER GAIN (PSID/PSID)

	Lot				Total
	A	B	C	D	
Sensor 1	3.33	2.98	3.14	3.52	
Sensor 2	3.26	3.16	3.24	3.05	
Sensor 3	3.37	2.99	3.38	3.38	
Sensor 4	3.57	3.36	3.55	3.06	
Sensor 5	3.80	3.39	3.24	---	
$\sum x_i$	17.33	15.88	16.55	13.01	62.77
$\bar{x}$	3.47	3.18	3.31	3.25	3.30
s^2	0.04813	0.03823	0.02530	0.05529	0.046469
s	0.219	0.196	0.159	0.235	0.216
95% C.I.	0.61	0.54	0.44	0.75	0.45
Interval	2.8 to 4.08	2.64 to 3.72	2.87 to 3.75	2.50 to 4.00	2.85 to 3.75

The variances between lots and within lots were calculated as follows:

$$\text{Correction Factor} = (\sum x_i)^2/N = 207.37226$$

$$\text{Crude Lot SS} = \sum_i (T_i^2/N_i) = \frac{(17.33)^2}{5} + \frac{(15.28)^2}{5} + \frac{(16.55)^2}{5} + \frac{(13.01)^2}{4}$$

$$= 207.59618$$

$$\text{Total SS} = \sum x_i^2 - (\sum x_i)^2/N = 208.2087 - 207.37226 = 0.8364$$

$$\text{Lot SS} = \sum_i (T_i^2/N_i) - (\sum x_i)^2/N = 207.59618 - 207.37226 = 0.2239$$

$$\text{Within Lot SS} = \text{Total SS} - \text{Lot SS} = 0.8364 - 0.2239 = 0.6125$$

The analysis of variance is summarized in Table B-25.

TABLE B-25. PID AMPLIFIER GAIN ANALYSIS OF VARIANCE

Source	SS	df	MS	Ratio	$F_{\alpha=0.05}$
Lots	0.2239	3	0.07463	1.83	3.29
Within Lot	0.6125	15	0.04083		
Total	0.8364	18	0.04647		

From Table B-25 it is seen that there is no significant difference between the variable within lots and the variance between lots at the 95-percent probability level.

The data in Table B-24 shows that the 95-percent confidence interval for the PID gain is 3.30 ±0.45. The specification of 3.4 ±0.5 is reasonable, and from the universe represented by this data, a yield of approximately 95 percent would be obtained.

PID Null Offset

The data for PID null offset is summarized in Table B-26.

TABLE B-26. PID AMPLIFIER NULL OFFSET (PSID AT OUTPUT)

	Lot				Total
	A	B	C	D	
Sensor 1	+0.10	-0.30	+0.20	+0.25	
Sensor 2	-0.25	+0.10	+0.15	+0.30	
Sensor 3	-0.25	---	0	+0.10	
Sensor 4	-0.10	---	-0.05	+0.10	
Sensor 5	---	---	-0.15	---	
$\sum x_i$	-0.50	-0.20	+0.15	+0.75	0.20
$\bar{x}$	-0.125	-0.100	+0.03	+0.1875	0.0133
s^2	0.02750	0.08000	0.02075	0.01062	0.03588
s	0.166	0.283	0.144	0.103	0.189
95% C.I.	0.53	3.60	0.40	0.33	0.40
Interval	-0.065 to +0.40	-3.70 to +3.50	-0.37 to +0.43	-0.14 to +0.52	-0.39 to +0.42

The lot-to-lot variance and between-lot variance were calculated in the following manner:

$$\text{Correction Factor} = (\sum x_i)^2/N = 0.0026667$$

$$\text{Total SS} = \sum x_i^2 - (\sum x_i)^2/N = 0.5050 - 0.0026667 = 0.50233$$

$$\text{Crude Lot SS} = \sum_i (T_i^2/N_i) = \frac{(-0.50)^2}{4} + \frac{(-0.20)^2}{2} + \frac{(0.15)^2}{5} + \frac{(0.75)^2}{4}$$

$$= 0.2276$$

$$\text{Lot SS} = \sum_i (T_i^2/N_i) - (\sum x_i)^2/N = 0.2276 - 0.0026667 = 0.22493$$

$$\text{Within Lot SS} = \text{Total SS} - \text{Lot SS} = 0.50233 - 0.22493 = 0.2774$$

Table B-27 summarizes the analysis of variance.

TABLE B-27. PID AMPLIFIER NULL OFFSET ANALYSIS OF VARIANCE

Source	SS	df	MS	Ratio	$F_{\alpha=0.05}$
Lot	0.22493	3	0.07498	2.97	3.59
Within Lot	0.2774	11	0.02522		
Total	0.50233	14	0.03588		

From Table B-27 it is seen that there is no significant difference between the lot-to-lot variance and the within-lot variance. The data appears to be normal.

Table B-26 shows that the 95-percent confidence interval for the PID null offset is 0.01 ±0.40 deg/sec. The specification of ±0.5 deg/sec will allow a greater than 95-percent yield in the universe represented by this data.

The extremely wide range shown in Lot B is due to the size of the sample and not to any significant change in variability. The value in the Student t table adjusts the standard deviation for sample size when dealing with small samples. The value at a 95-percent probability level is 1.96 when the sample size reaches infinity. However, for a sample of 5, this value increases to 2.776, and for a sample of 2, this value increases to 12.706. For this reason, a sample of 2 does not give a very reliable estimate of confidence intervals.

Throughout this report, projected yields have been based only on the raw data for the parameters shown. Some decrease in yield is to be expected due to catastrophic failures; i.e., dropping a part on the floor, losing a part in process, or grinding a surface too thin. In addition to these failures, some parts will be scrapped due to properties not evaluated in this statistical study; i.e., linearity, curve shape, etc.

On the basis of overall considerations, a yield of 80 to 85 percent is indicated by this study.

Due to the fact that the current process has a reasonable yield of parts within specification, no fractional factorial or factorial experiments were carried out. In the event that the process gets out of control when larger production is under way, planned experiments of this type may be needed to set limits on various process variables.

End 5-77

4093-77